NASA CONTRACTOR
REPORT

Report No. 61281

SPACE RADIATION HAZARDS TO PHOTOGRAPHIC FILM IN THE APOLLO TELESCOPE MOUNT AND ORBITING WORKSHOP

By C. W. Hill, D. N. Davis, and H. K. Parker, Jr.

Lockheed-Georgia Company
Marietta, Georgia 30060

May 1969

Final Report

Prepared for

NASA-GEORGE C. MARSHALL SPACE FLIGHT CENTER
Marshall Space Flight Center, Alabama 35812

TECHNICAL REPORT STANDARD TITLE PAGE

1. Report No. NASA CR-61281	2. Government Accession No.	3. Recipient's Catalog No.
4. Title and Subtitle SPACE RADIATION HAZARDS TO PHOTOGRAPHIC FILM IN THE APOLLO TELESCOPE MOUNT AND ORBITING WORKSHOP		5. Report Date May 1969 6. Performing Organization Code
7. Author(s) C. W. Hill, D. N. Davis, and H. K. Parker, Jr.		8. Performing Organization Report No. ER 10156
9. Performing Organization Name and Address Lockheed-Georgia Company Marietta, Ga. 30060		10. Work Unit No. 11. Contract or Grant No. NAS 8-21266 13. Type of Report and Period Covered Final
12. Sponsoring Agency Name and Address George C. Marshall Space Flight Center Marshall Space Flight Center, Ala. 35812		14. Sponsoring Agency Code

15. Supplementary Notes

16. Abstract

A mathematical model of the AAP cluster geometry has been constructed. Space radiation doses to Apollo Telescope Mount (ATM) photographic film and other experiment film throughout the cluster are computed. Radiation fogging density is estimated for the ATM film, and film degradation is found to be within tolerance limits.

17. Key Words	18. Distribution Statement
	FOR PUBLIC RELEASE Matt O. Buncell

19. Security Classif. (of this report)	20. Security Classif. (of this page)	21. No. of Pages	22. Price
U	U	62	

FOREWORD

This technical report is submitted to the Space Sciences Laboratory (SSL), George C. Marshall Space Flight Center, NASA, Huntsville, Alabama, according to the requirements of Contract NAS8-21266. The Contract Technical Monitor is M. O. Burrell of SSL.

The data utilized in this study were generated in several NASA centers, industrial facilities, and university and AEC laboratories. Nearly one hundred individuals were consulted during the contract effort. While it is impossible to list all contributors, their assistance is gratefully acknowledged.

TABLE OF CONTENTS

LIST OF TABLES AND FIGURES

LIST OF TABLES AND FIGURES
(Continued)

ABBREVIATIONS

AAP	Apollo Applications Program
AM	Airlock Module, between OWS and MDA
AS&E	American Science and Engineering Corporation
ATM	Apollo Telescope Mount
CM	Apollo Command Module
CMG	Control Moment Gyro
CPSM	Crew Provisions and Stowage Module
CSM	CM plus SM
EVA	Extra-Vehicular Activity
GSFC	Goddard Space Flight Center, NASA
HAO	High Altitude Observatory
HCO	Harvard College Observatory
LM	Lunar Module
MDA	Multiple Docking Adaptor
MIT	Massachusetts Institute of Technology
MSC	Manned Spacecraft Center, NASA
MSFC	Marshall Space Flight Center, NASA
NASA	National Aeronautics and Space Administration
NRL	Naval Research Laboratory
ORNL	Oak Ridge National Laboratory
OWS	Orbiting Work Shop, a converted SIV B stage
RACK	LM descent stage structure
SIV B	Third stage of the Saturn V and second stage of the Saturn IB
SLA	Spacecraft - LM Adapter, an aerodynamic, loadbearing shroud
SM	Apollo Service Module
SSL	Space Sciences Laboratory, MSFC
STS	Structural Transition Section, between MDA and AM

1.0 INTRODUCTION

Several of the experiments planned for the Apollo Applications Program require photographic film for the recording of data. This film comprises diverse types, each more or less sensitive to the particulate radiations found in space. The present study is an attempt to assess the radiation environment within the AAP cluster so that a determination of radiation damage to the film and consequent loss of data may be made.

The AAP film degradation problem encompasses several challenging aspects. The free space radiation environment must be estimated for the particular orbital parameters of interest. This radiation must then be transported through a conglomerate structure to a particular film. Finally, the effects of the penetrating radiation upon the film must be assessed.

This study concentrates upon the second phase of the problem, radiation transport through the complex configuration using the LSVDC4 program system[3]. Phase one, specification of the radiation environment, is based upon the Vette model[12] of the trapped radiation belts and is provided by J. W. Watts and M. O. Burrell[11] of Space Sciences Laboratories (SSL), MSFC. Phase three, radiation effects upon film, is evaluated for the Apollo Telescope Mount (ATM) films and is based upon data analyses of Kodak[4] and SSL[9,10].

A study summary and recommendations are given in Section 2. The radiation environment is discussed in Section 3. Section 4 presents results obtained during the study. Appendix A briefly describes the radiation transport programs utilized in the study and Appendix B illustrates the AAP cluster geometry model. Appendix C discusses the effects of radiation upon photographic film of concern to the ATM project.

2.0 SUMMARY AND RECOMMENDATIONS

Relatively good geometry models of the Apollo Telescope Mount (ATM), Crew Provisions and Stowage Module (CPSM), Multiple Docking Adapter (MDA), and Structural Transition Section (STS) have been constructed. The Airlock Module (AM) geometry model is incomplete. Simplified models of the Lunar Module (LM), Command and Service Modules (CSM), and Orbiting Work Shop (OWS) used in earlier studies are incorporated herein.

Dose estimates are presented for ATM films in the CPSM, ATM, and CM. Dose rates in the CPSM and ATM are comparable to each other, while dose rates in the CM are much lower. Therefore, films exposed early in the mission which are then stored in the CM receive relatively low doses. Estimates of radiation fogging density are made for each ATM film. All density estimates are below currently proposed limits. In particular, radiation fogging densities for the first load of film are low enough to consider substitution of faster, more radiation-sensitive films subject to confirmation of low CM dose rates and acceptance of the CM as a storage location for exposed ATM film.

Dose rate estimates are presented for 14 locations in the CM, MDA, STS, AM, and OWS to aid in selection of other photographic film storage sites. No self-shielding of the film repositories is considered; therefore, only relative comparisons may be made among the various locations. Comparisons are subject to change as additional geometric details are included in the AAP cluster geometry model. Radiation fogging density estimates for these films are not made in the present study; these estimates depend upon refinement of the geometry model, selection of film types, and experimental determination of film degradation due to radiation exposure.

The experience and results gained in the present study suggest the desirability of additional effort in several areas. These recommendations are as follows:

- Refinement of several ATM telescope and camera geometry models when detailed data become available,
- Minor additions to ATM geometry model as suggested in Appendix B,
- Adaptation of existing LM and Block II Apollo CM geometry models to the LSVDC4 program system,
- Revision of the AM and OWS geometry models when data become available,
- Additional space and time mapping of ATM film doses in all locations,
- Incorporation of film repository model for non-ATM films and recalculation of dose rates,
- Calculation of non-ATM film degradation as data become available,
- Examination of effects of radiation flux anisotropy.

3.0 RADIATION ENVIRONMENT

The AAP cluster will follow a circular orbit at altitudes between 180 and 220 nautical miles and at an inclination between 30° and 35°. This orbit is relatively radiation-free except when it intersects the South Atlantic magnetic anomaly. Six to ten times per day, the spacecraft encounters a highly anisotropic radiation flux - primarily protons - for periods of five to ten minutes (see Figure 3-1). The cosmic ray background and radiation from solar flux events are not major contributors to the radiation problem due to the shielding afforded by the Earth's magnetic field.

The radiation environment over a range of possible orbits has been computed by Watts and Burrell[11] of MSFC using the Vette model[12] of the trapped radiation belts. The consequences of varying orbital parameters may be seen in Figures 3-2 and 3-3. The dose rate is computed inside spherical shell aluminum shields for various thicknesses.

A circular orbit of 210 nautical miles and 35° inclination is the present choice for the AAP mission. The proton and electron fluxes, averaged over many orbits, are given in Table 3-1. The dose rate behind spherical shell aluminum shields due to this environment is shown in Figure 3-4.

The omnidirectional proton fluxes listed in Table 3-1 are thought to be correct within a factor of two. Flux intensities constitute a major uncertainty in the present results. A second uncertainty arises from the interaction of the anisotropic flux with the complex shield configuration. Protons in the anomaly are near their mirror points so their trajectories are nearly flat spirals. Therefore, the flux appears to impinge upon the sun-oriented cluster from directions nearly perpendicular to the local magnetic field vector. Several factors tend to smear this distribution to some extent. The present study approximates the true angular distribution with an isotropic distribution.

Electron doses at the most exposed film detectors in the ATM and CPSM are less than one per cent of the proton doses for low orbits and inclinations. Bremsstrahlung doses are

smaller still. These dose components are, therefore, neglected in the present study. The electron problem may be significant for orbits with angles of inclination greater than 40°.

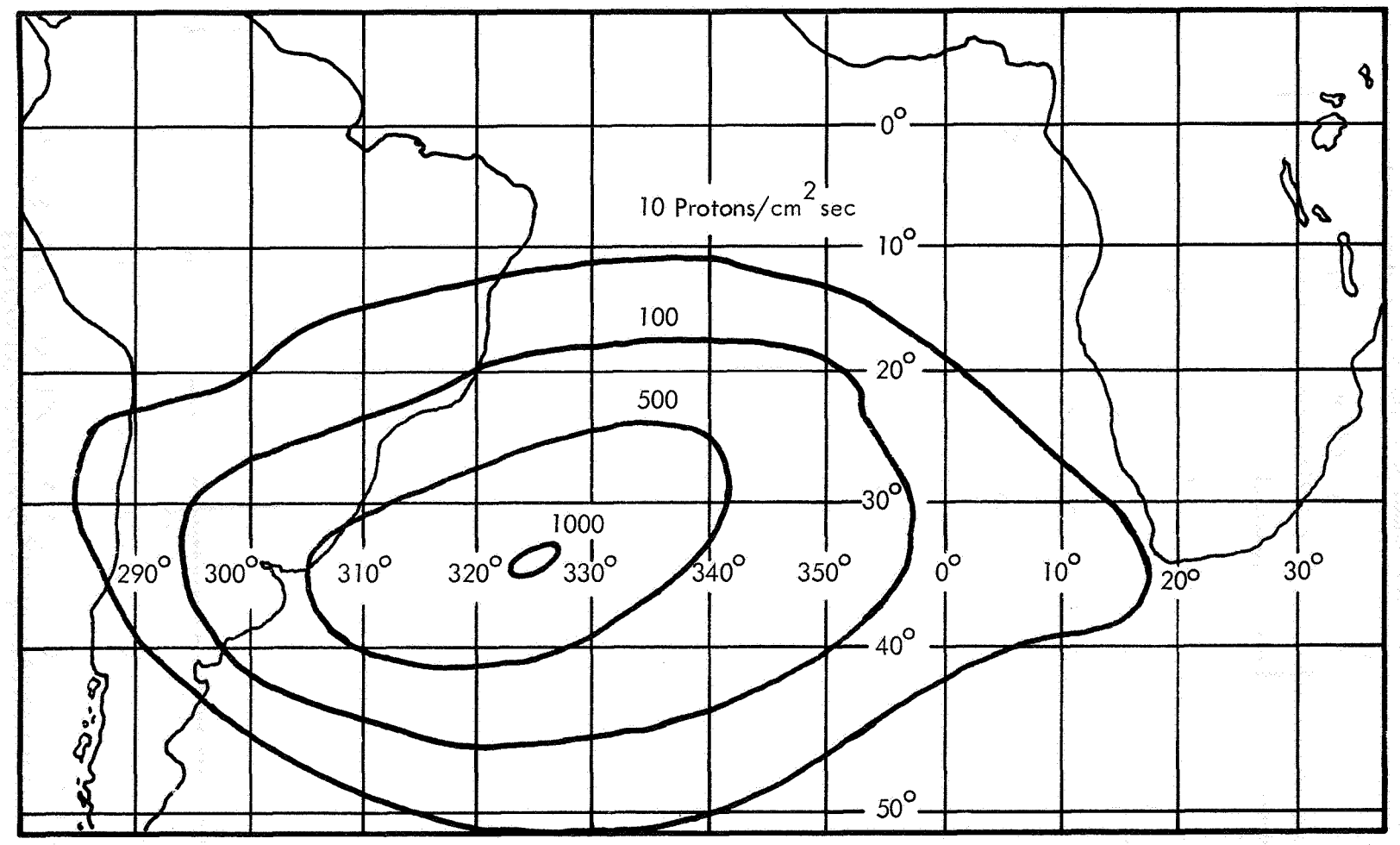

Altitude = 240 Nautical Miles
Vette's Proton Data AP1

FIGURE 3-1 AN ISOFLUX PLOT FOR PROTONS WITH ENERGIES GREATER THAN 34 MeV IN THE SOUTH ATLANTIC ANOMALY AT AN ALTITUDE OF 240 NAUTICAL MILES (444 km)

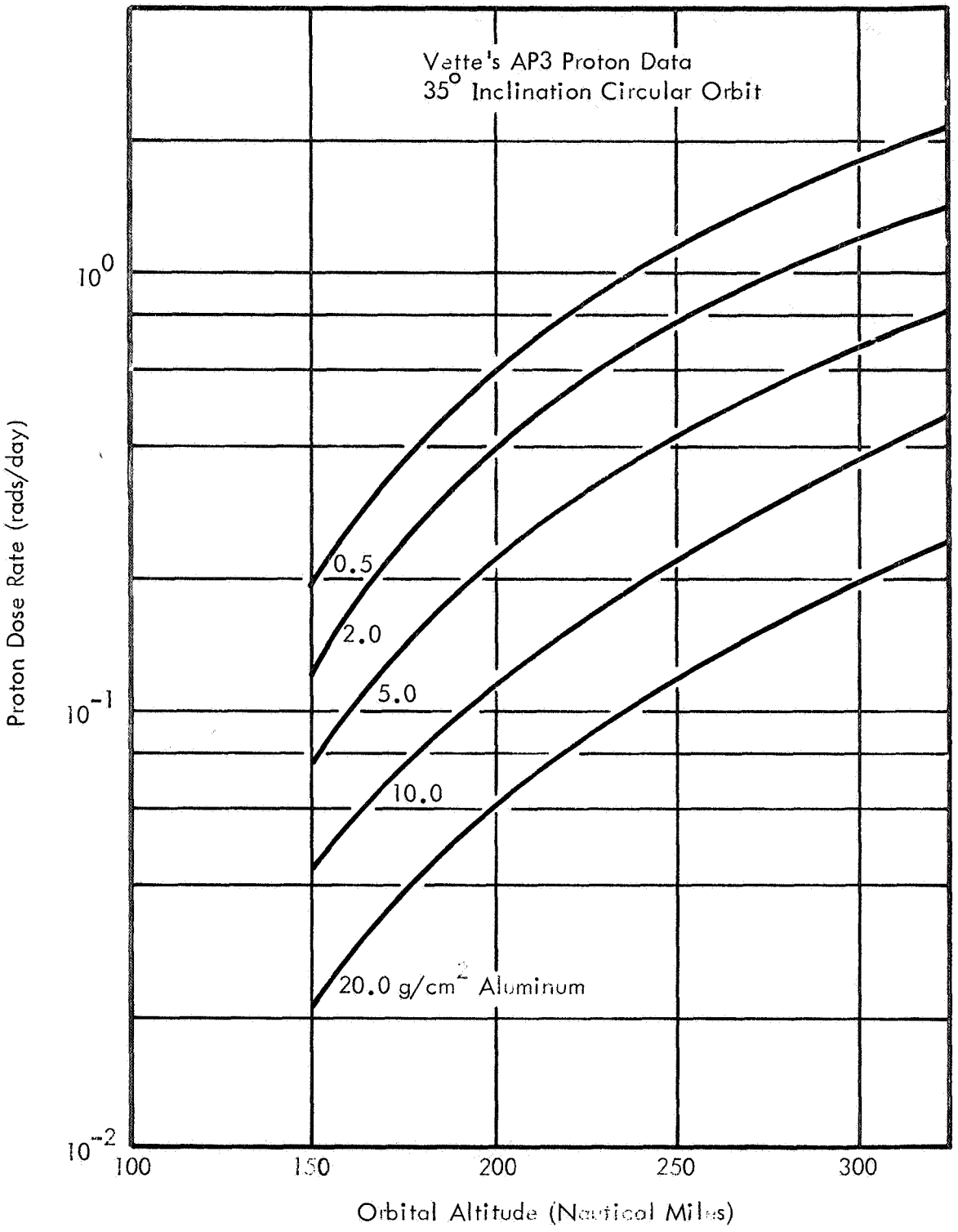

FIGURE 3-2 PROTON DOSE VERSUS ALTITUDE FOR VARIOUS SHIELD THICKNESSES AT 35° ORBITAL INCLINATION

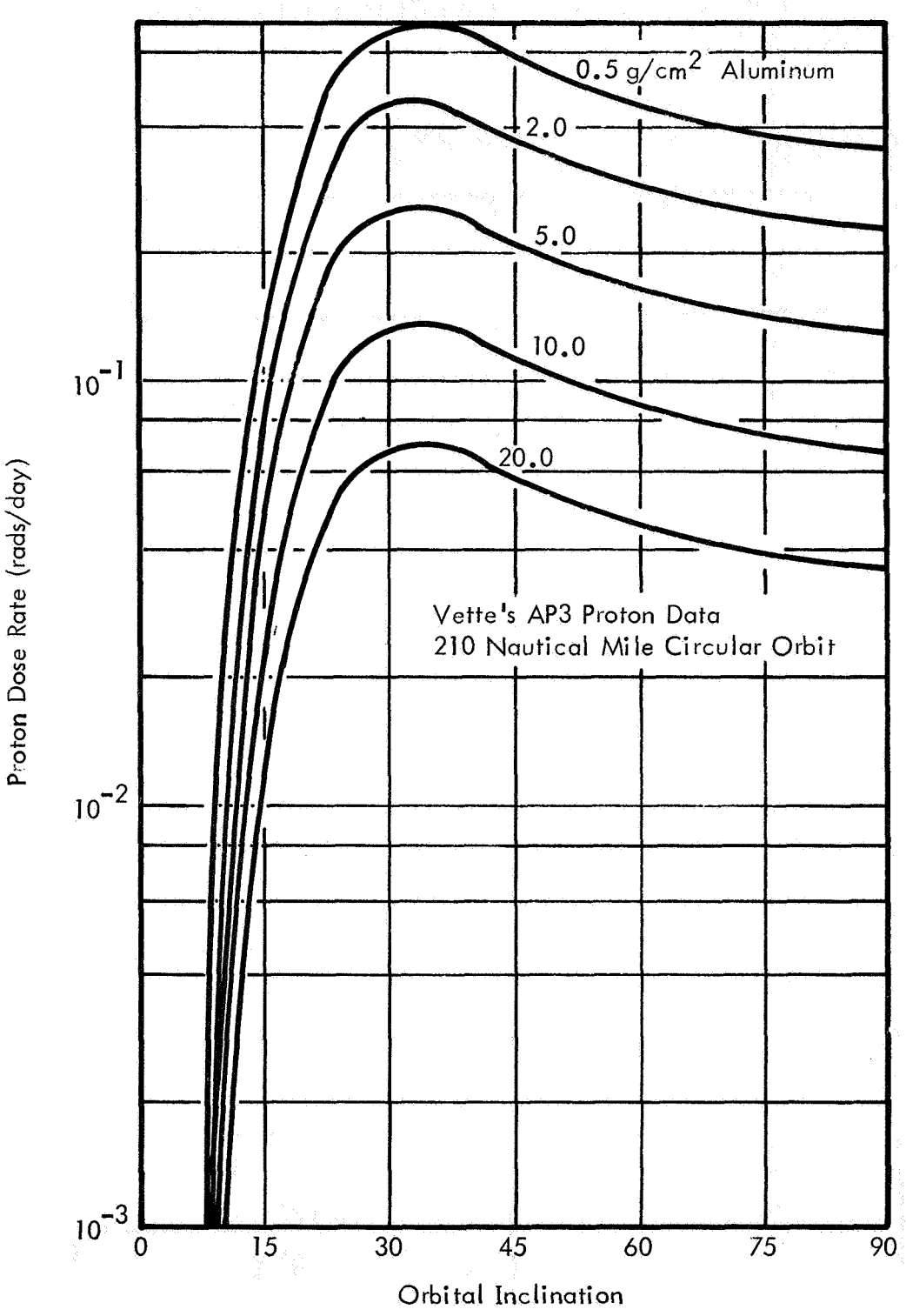

FIGURE 3-3 PROTON DOSE VERSUS INCLINATION FOR VARIOUS SHIELD THICKNESSES AT 210 NAUTICAL MILES (389 km)

TABLE 3-1 ATM ORBIT RADIATION ENVIRONMENT

PROTON

E (MeV)	Flux (p/cm^2-MeV-day)
10.0	69000
42.5	33200
90.0	14200
150.0	5660
300.0	744
1000.0	2.6

ELECTRON

E (MeV)	Flux (e/cm^2-MeV-day)
10^{-4}	2.618×10^{11}
0.25	3.469×10^{10}
0.50	4.673×10^{9}
1.00	7.499×10^{7}
1.50	1.078×10^{6}
2.00	9.008×10^{5}
4.00	5.637×10^{5}
6.50	3.261×10^{5}
10.00	1.516×10^{5}

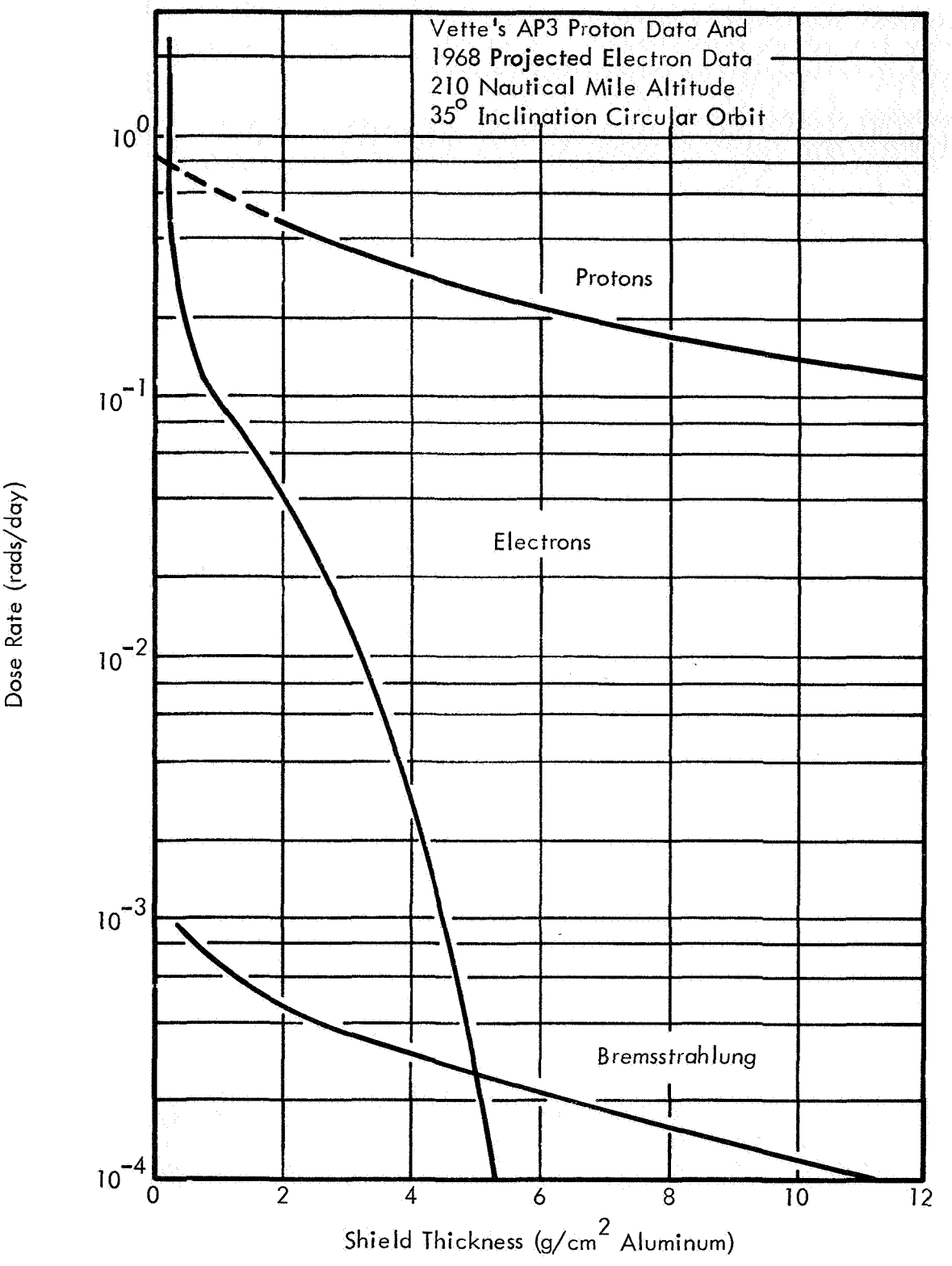

FIGURE 3-4 DOSE VERSUS SHIELD THICKNESS FOR PROTONS, ELECTRONS AND BREMSSTRAHLUNG IN A 210-NAUTICAL MILE (389 km), 35° CIRCULAR ORBIT

4.0 RESULTS

The results of the dose estimates computed during the present study are detailed in this section. The first part includes dose estimates for ATM film in the launch storage location, CPSM; the experiment location, ATM; and the return storage location, Apollo CM. The second part of this section includes dose rate estimates for potential storage locations of OWS experiment film throughout the AAP2 cluster.

4.1 ATM FILM RADIATION EXPOSURE

The AAP 3/4 cluster configuration is outlined in Figure 4-1. The AAP 3 Apollo CM is docked into the axial MDA port and the AAP 4 LM is docked into the MDA radial port I. The ATM contains eight telescopes, six of which require film. Four camera loads are provided for each of the six film-using telescopes. One camera load of each type is launched in operating position aboard the ATM. Three replacement cameras of each type are launched in the AAP 4 CPSM. After a set of ATM cameras is exposed, astronaut EVA replaces the used cameras and returns them to the CM. Dose estimates are presented for each location.

4.1.1 CPSM Radiation Exposure

The CPSM is positioned around the LM docking tunnel as shown in Figure 4-2. A cross-section view of the CPSM is shown in Figure 4-3. Individual cameras are labeled according to responsible experiment organization or function, and order of usage (Arabic numerals). The NRL A and B 4 boxes are empty cassettes provided for the NRL cameras launched on the ATM.

The number 3 cameras and the empty NRL 4 cassettes are removed during the first EVA, approximately 14 days after mission start. The number 2 cameras are removed and placed on the ATM two weeks later. The number 1 cameras are removed after another two weeks.

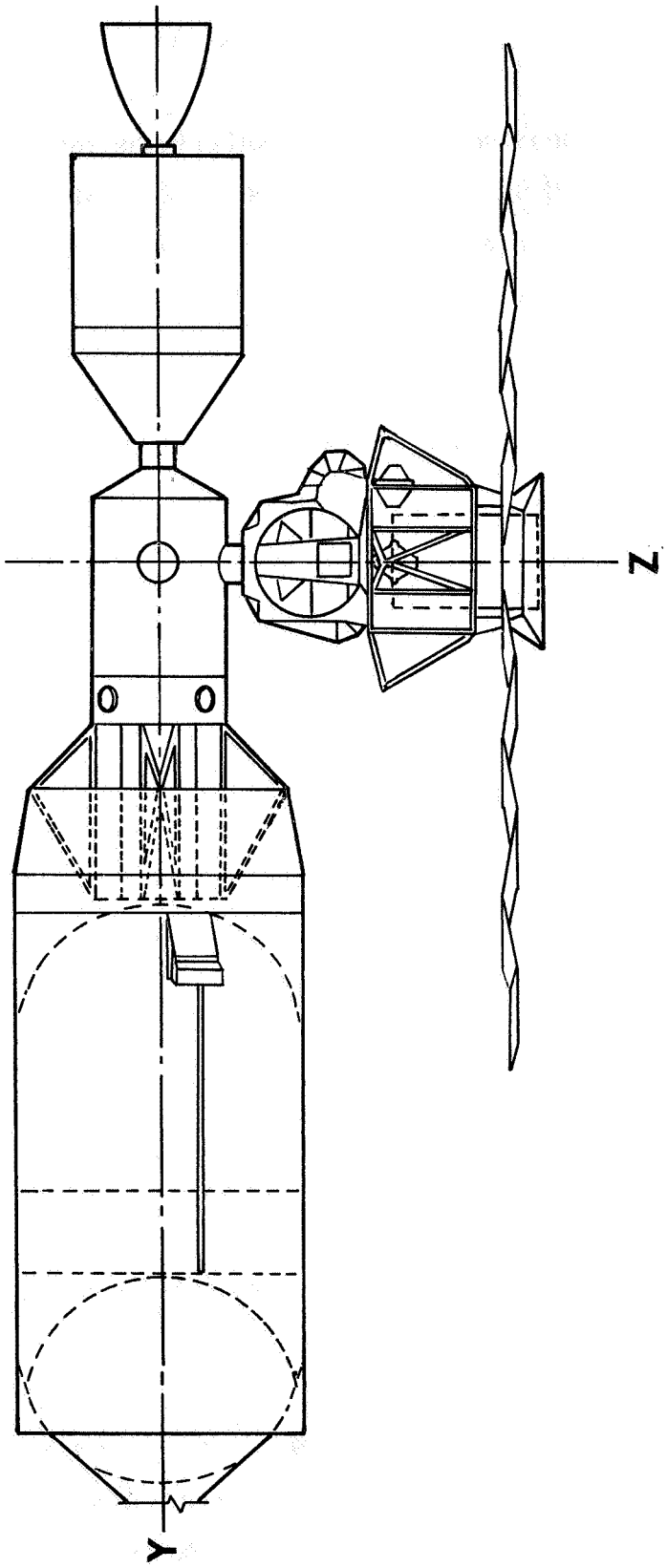

FIGURE 4-1 AAP 3/4 CLUSTER CONFIGURATION

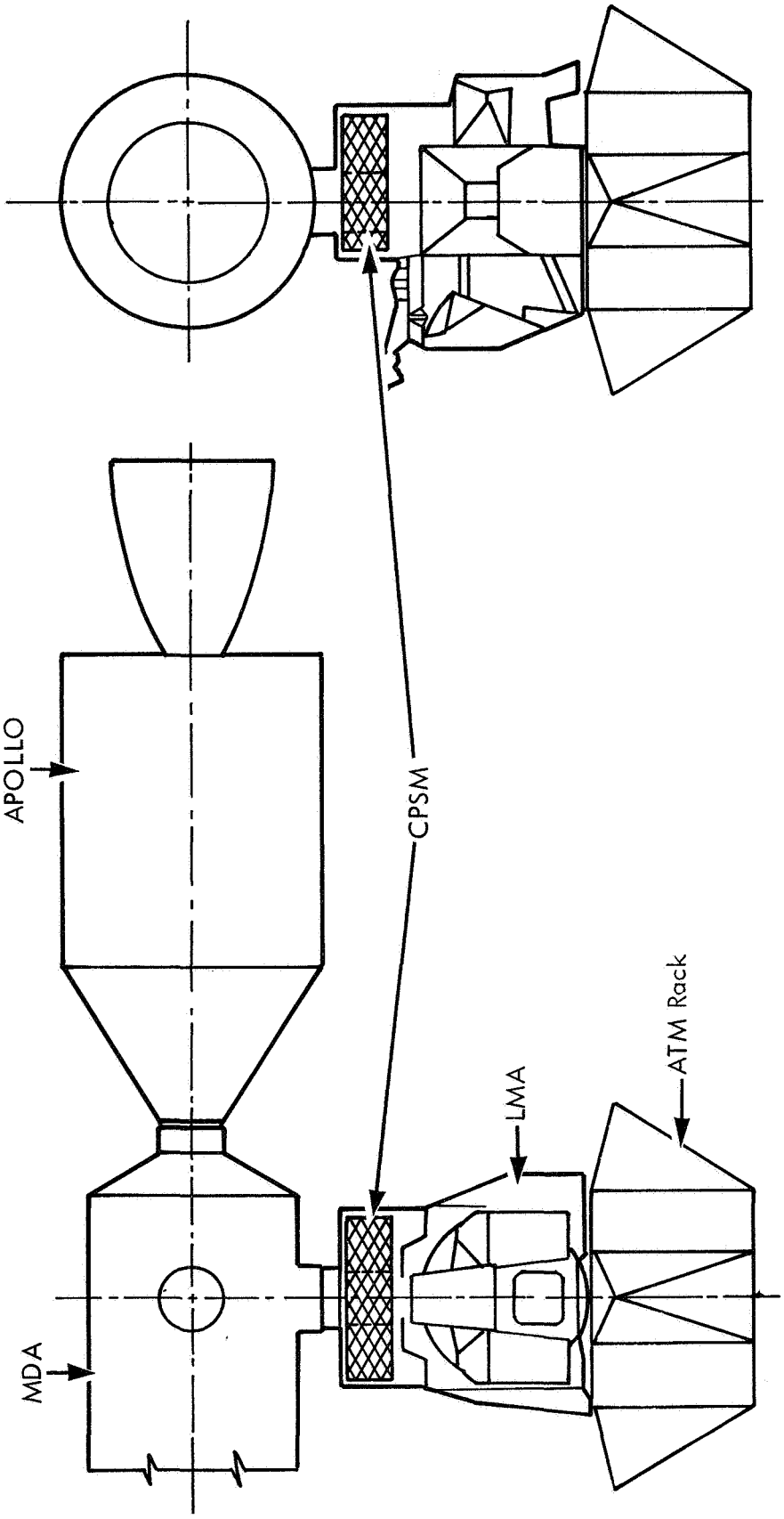

FIGURE 4-2 CPSM LOCATION

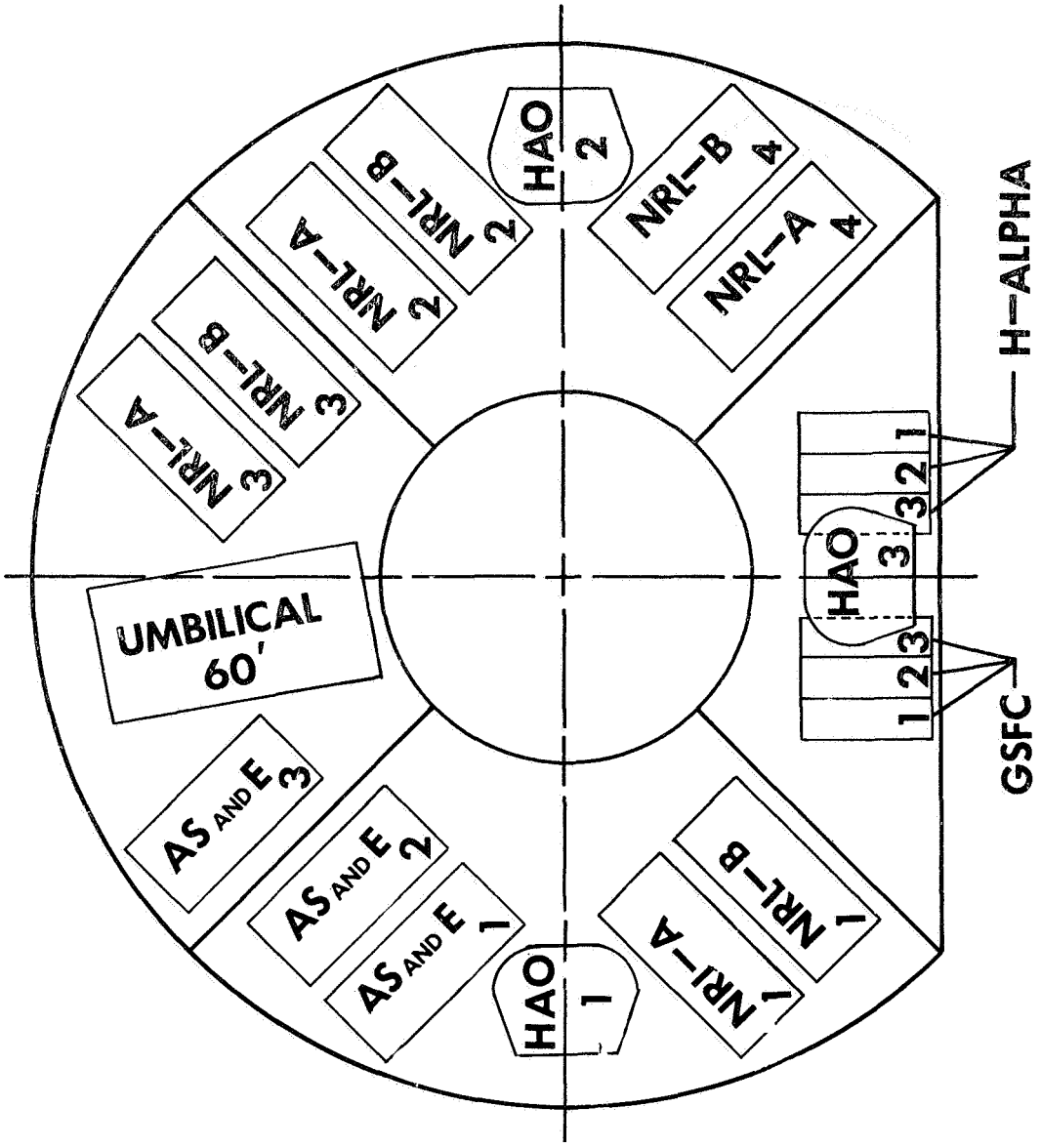

FIGURE 4-3 CPSM BASE LINE STOWAGE

The geometry models used to simulate cameras and film are discussed in Appendix B. The GSFC camera, developed by the Astrionics Laboratory at MSFC, is used in the GSFC and H-Alpha 1 experiments. It is also placed in the HAO experiment in the present study due to lack of better data. It is estimated that the GSFC and H-Alpha 1 camera models are good; the AS&E and NRL camera models are fair, but conservative; and the HAO camera model is poor and quite conservative.

Radiation exposure estimates are made for "worst case" cameras which spend 42 days in the CPSM and the remaining 14 days of the 56 day mission on the ATM. Detectors are placed 0.1 inches inside the film surfaces near a film edge, except for an additional GSFC detector buried deep inside the film.

A total of 180 vectors scans the configuration around each detector. Additional detail is not warranted at this time due to the relatively simple nature of the LM model. H-Alpha 1 exposure estimates are assumed to be the same as those for the GSFC camera. Cumulative CPSM exposure estimates are shown in Table 4-1.

4.1.2 ATM Radiation Exposure

The location of experiment telescopes in the ATM canister is indicated in Figure 4-4. The GSFC, H-Alpha 1, and AS&E cameras are located on the LM end of the telescopes. The HAO camera is positioned on the outboard side of the HAO optical housing near the LM end of the spar. The NRL cameras are found near the sun end of their telescopes.

Two detectors are placed in each camera. In the spool-type cameras, the film is on the supply reel. The first detector is buried 0.1 inches within the film near the forward face of the camera. The second detector is 0.1 inches within the film near the middle of the film roll. In the slide-type (NRL) cameras, the detectors are positioned 0.1 inches from the top of the top deck of slides and 0.1 inches from the bottom of the bottom deck of slides. Both detectors are 0.1 inches within the slide decks opposite the aperture, i.e.,

TABLE 4-1 RADIATION DOSE ESTIMATES ON CPSM

(215 Nautical Miles, 35 Degree Orbit)

Dose (Rad Air)

Camera	Time (Days)		
	14	28	42
GSFC (Inside)	0.82	1.73	2.99
GSFC	1.05	2.22	3.81
HAO	1.35	2.71	4.09
H-ALPHA 1[1]	1.05	2.22	3.81
AS&E	1.93	3.87	5.83
NRL-A	1.99	3.98	5.99
NRL-B[2]	1.99	3.98	5.99

Notes:

1. H-ALPHA 1 assumed to be same as GSFC.
2. NRL-B assumed to be same as NRL-A.

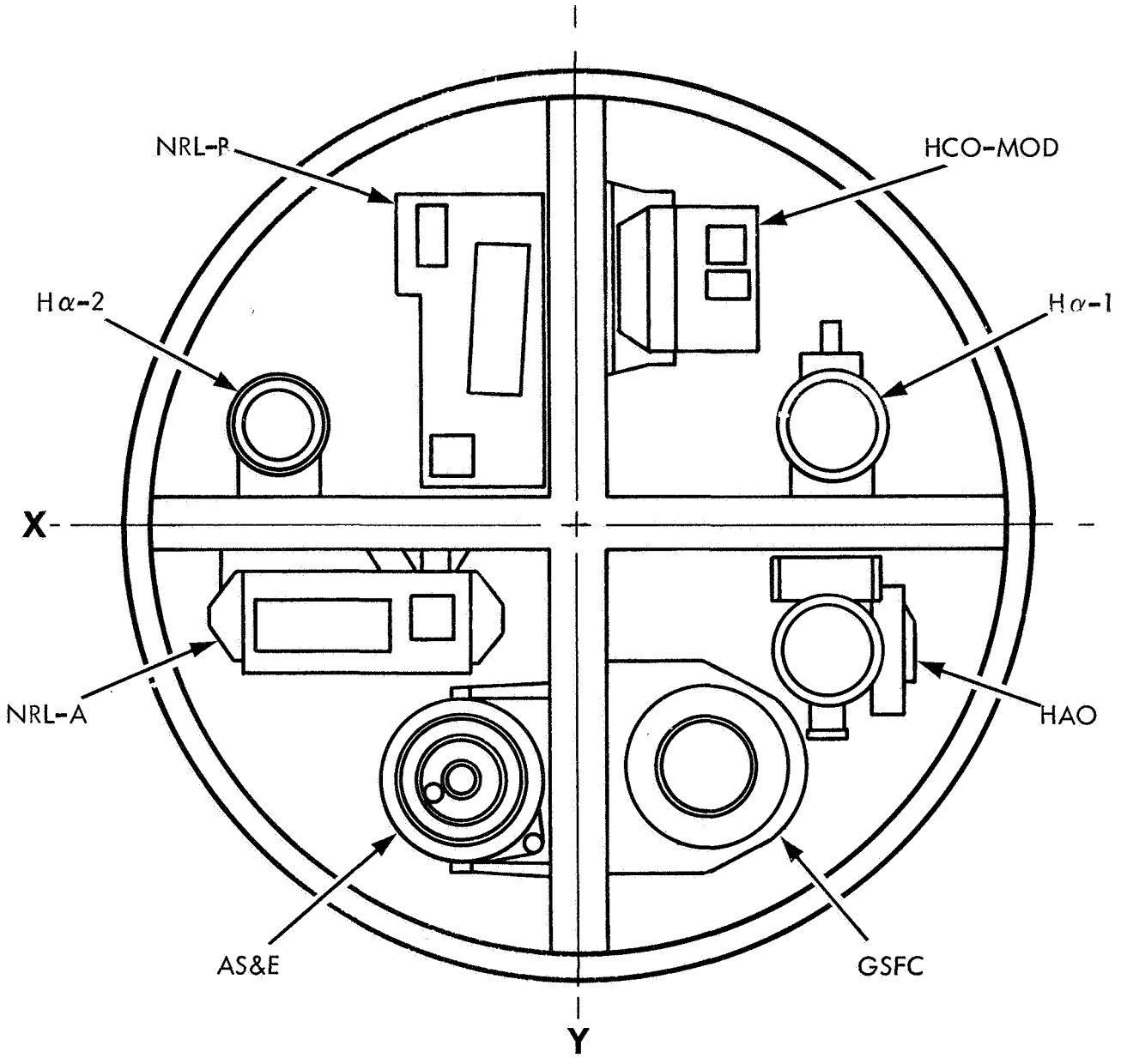

FIGURE 4-4 ATM CANISTER (SUN END)

the most exposed location. Thus, all exposure estimates should be somewhat conservative. A total of 972 vectors scans the geometry around each detector. Computed ATM dose estimates are given in Table 4-2.

4.1.3 CM Radiation Exposure

The location of ATM cameras in the Apollo CM is depicted in Figure 4-5. This arrangement is arbitrary; no suggestion of eventual ATM camera positions is implied. A single set of cameras is considered because it represents the "worst case".

Two detectors are placed in each camera in the same relative positions considered in the ATM locations. A total of 180 vectors scans the configuration around each detector. Radiation exposure estimates are shown in Table 4-3.

4.1.4 ATM Film Degradation

This section combines the preceding radiation exposure estimates with a simplified time line schedule and the film degradation data of Appendix C to arrive at ATM film degradation estimates. The purpose of this procedure is to determine the degree of radiation fogging to be expected so that little loss of data due to radiation is assured. Tentatively, a radiation-induced density of 0.2 has been selected as an upper limit which will not seriously degrade the quality of the data.

The ATM film is divided into four sets or loads. Each load contains one camera for each of the six film-using telescopes. The first load is launched on the ATM; the other three in the CPSM. After a two week period the film on the ATM is stored in the CM and is replaced by a fresh load from the CPSM. This cycle continues until all the film is exposed.

The dose rate increase in the CPSM due to removal of cameras is considered. However,

TABLE 4-2 RADIATION DOSE ESTIMATES ON THE ATM

(215 Nautical Miles, 35 Degree Orbit)

Dose (Rad Air Per 14 Days)

Camera	Detector I	Detector II
GSFC	0.92	0.75
HAO	1.26	1.23
H-ALPHA 1	0.79	0.70
AS&E	0.67	0.66
NRL-A	2.02	1.79
NRL-B	1.21	1.47

TABLE 4-3 RADIATION DOSE ESTIMATES IN THE APOLLO CM

(215 Nautical Miles, 35 Degree Orbit)

Dose (Rad Air Per 14 Days)

Camera	Detector I	Detector II
GSFC	0.35	0.33
HAO	0.28	0.28
H-ALPHA 1	0.34	0.32
AS&E	0.32	0.31
NRL-A	0.42	0.36
NRL-B	0.35	0.33

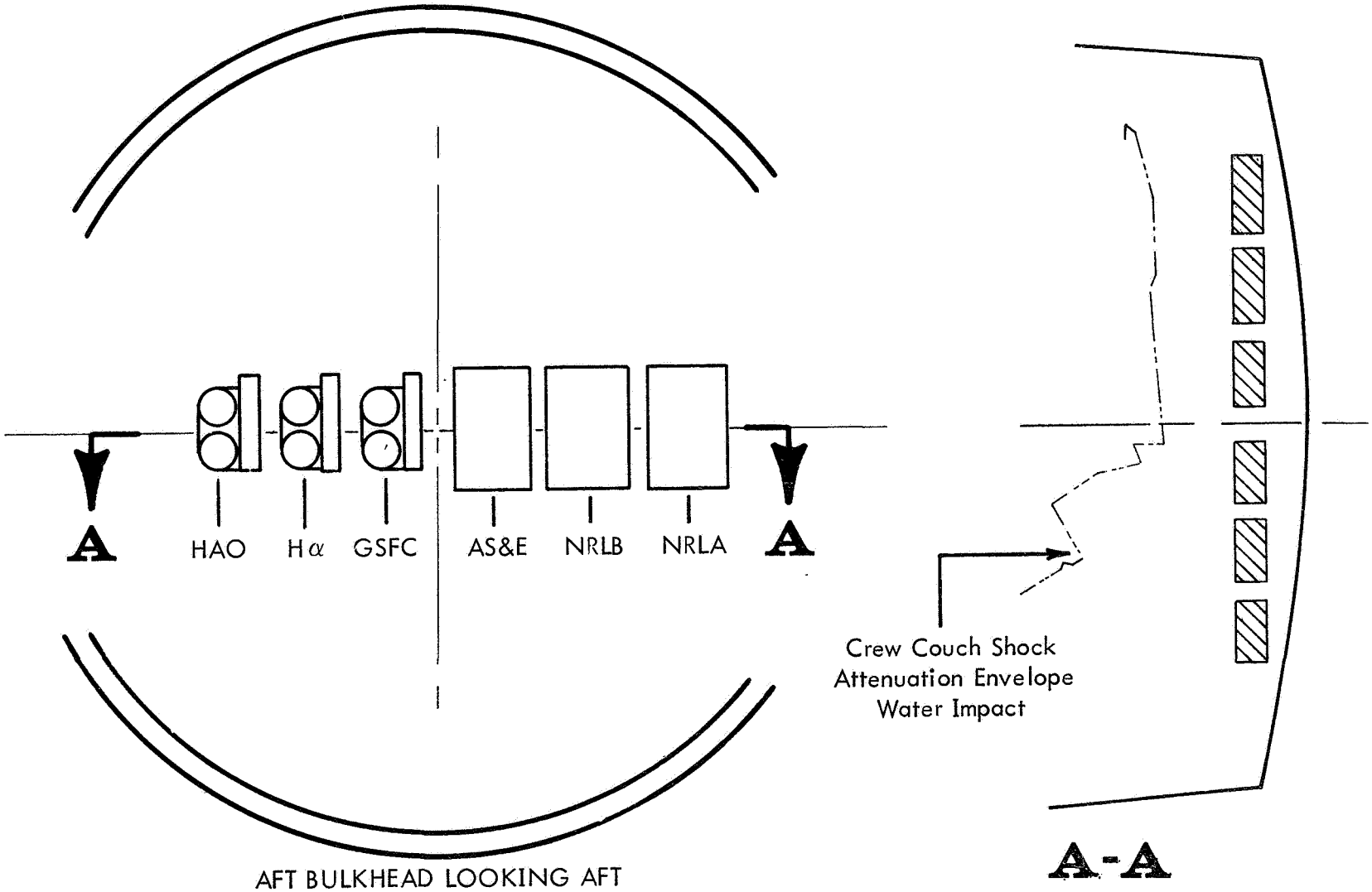

AFT BULKHEAD LOOKING AFT

FIGURE 4-5 CM CAMERA STOWAGE

the dose rate decrease in the CM due to other sets of cameras is ignored. Thus, conservative choices were made where possible. In those cases where two detector points are considered, density estimates are given for the first one.

Typical values of radiation dose and fogging density for each film in each load are given in Table 4-4. The dose rates are comparable on the CPSM and ATM except for the AS&E film where the CPSM dose rate is three times higher. The CM dose rates are two to five times lower than the CPSM and ATM dose rates. These estimates are subject to some uncertainty due to incomplete mapping over the film and simplifications in the geometric models, particularly the CM and LM.

The density estimates show that all films possess some safety margin under the currently proposed limit of 0.2. No attempt has been made to include temperature-induced film darkening which may be significant for some films. Note that densities for the first load are approximately one third those for the fourth load; densities for the second load are one half those for the fourth. These facts suggest that faster, more radiation sensitive films might be launched aboard the ATM as the first load should their increase in data-gathering capability warrant increased mission complexity. Such a decision should be confirmed by a refined analysis of the CM geometry because present estimates yield rather large effective shield thicknesses of 28 to 36 gm/cm^2 (including self - and mutual shielding).

4.2 OWS FILM RADIATION EXPOSURE

The AAP 2 cluster configuration is illustrated in Figure 4-6. The AAP 2 Apollo CM is docked into the MDA axial port. The ATM/RACK is not present during this mission. Nevertheless, a large quantity of photographic film will be used in OWS experiments and other activities. A preliminary radiation environment survey is made at 14 locations in the cluster. The results of this survey are shown in Table 4-5.

LOAD ONE						
Location		CPSM	ATM	CM	Mission Dose	Density
Dwell Time - Days		0	14	42		
Camera	Film	Dose - Rad (Air)				
GSFC	Pan-X		0.92	1.05	1.97	.035
HAO	Pan-X		1.26	0.84	2.10	.040
Hα-1	SO-375		0.79	1.02	1.81	.008
AS&E	Pan-X		0.67	0.94	1.61	.027
NRL-A	SWR		2.02	1.26	3.28	.030
NRL-B	SWR		1.21	1.05	2.26	.020

LOAD TWO						
Location		CPSM	ATM	CM	Mission Dose	Density
Dwell Time - Days		14	14	28		
Camera	Film	Dose - Rad (Air)				
GSFC	Pan-X	1.05	0.92	0.70	2.67	.048
HAO	Pan-X	1.35	1.26	0.56	3.17	.058
Hα-1	SO-375	1.05	0.79	0.68	2.52	.011
AS&E	Pan-X	1.93	0.67	0.64	3.24	.059
NRL-A	SWR	1.99	2.02	0.84	4.85	.045
NRL-B	SWR	1.99	1.21	0.70	3.90	.035

TABLE 4-4 ATM FILM DOSES AND RADIATION FOGGING DENSITIES

LOAD THREE						
Location		CPSM	ATM	CM	Mission Dose	Density
Dwell Time - Days		28	14	14		
Camera	Film	Dose - Rad (Air)				
GSFC	Pan-X	2.22	0.92	0.35	3.49	.062
HAO	Pan-X	2.71	1.26	0.28	4.25	.080
Hα-1	SO-375	2.22	0.79	0.34	3.35	.018
AS&E	Pan-X	3.87	0.67	0.32	4.86	.096
NRL-A	SWR	3.98	2.02	0.42	6.42	.061
NRL-B	SWR	3.98	1.21	0.35	5.54	.051

LOAD FOUR						
Location		CPSM	ATM	CM	Mission Dose	Density
Dwell Time - Days		42	14	0		
Camera	Film	Dose - Rad (Air)				
GSFC	Pan-X	3.81	0.92		4.73	.093
HAO	Pan-X	4.09	1.26		5.35	.110
Hα-1	SO-375	3.81	0.79		4.60	.022
AS&E	Pan-X	5.83	0.67		6.50	.140
NRL-A	SWR	5.99	2.02		8.01	.076
NRL-B	SWR	5.99	1.21		7.20	.067

TABLE 4-4 ATM FILM DOSES AND RADIATION FOGGING DENSITIES
(Continued)

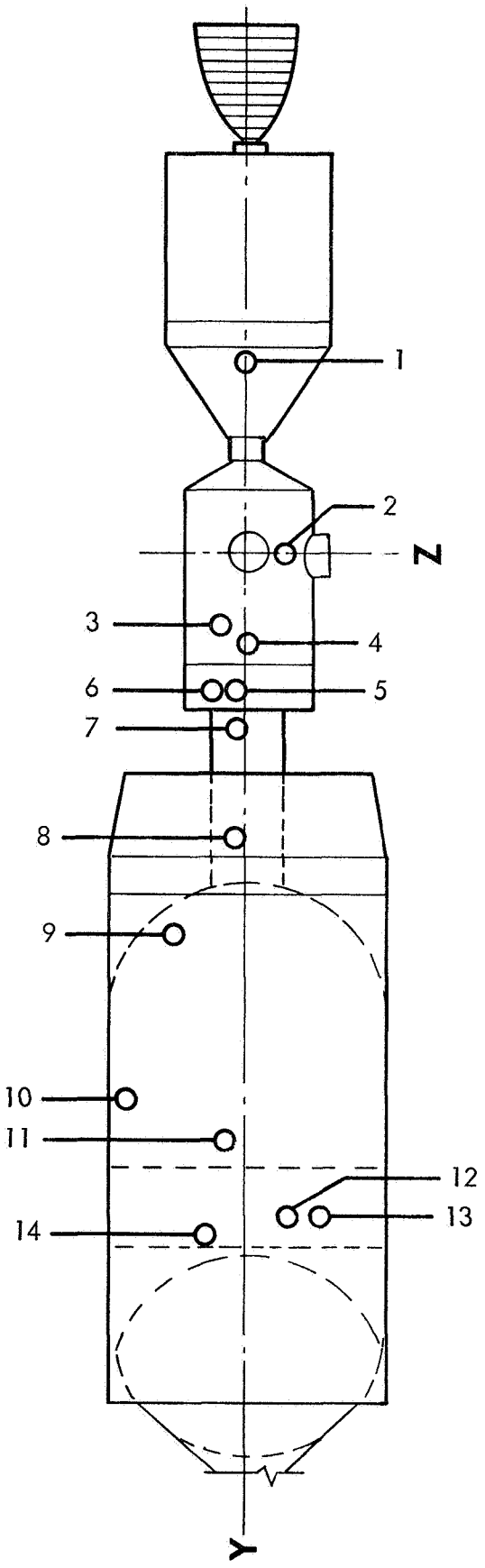

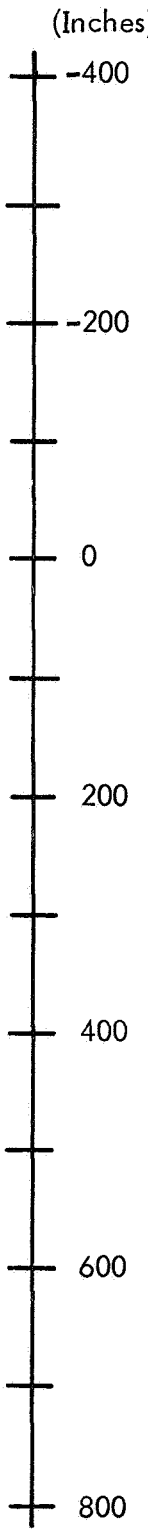

FIGURE 4-6 AAP-2 CONFIGURATION

TABLE 4-5 FILM REPOSITORY DOSE RATE ESTIMATE

Detector	Location	X	Y	Z	Proton Dose Rate (Rad(Air)/Day)
1	CM	0.0	-160.0	0.0	0.059
2	MDA	0.0	0.0	27.5	0.186
3	MDA	-20.5	71.0	-20.5	0.159
4	MDA	28.0	95.3	0.0	0.197
5	STS	37.21	123.03	-21.5	0.291
6	STS	-32.8	123.03	-36.4	0.297
7	AM	-16.7	163.03	-17.28	0.268
8	AM	-17.81	233.03	-11.11	0.281
9	OWS	0.0	364.24	-40.0	0.341
10	OWS	-45.0	519.74	-111.0	0.383
11	OWS	-45.7	563.44	-14.81	0.457
12	OWS	-66.5	628.74	21.6	0.415
13	OWS	-40.7	628.74	73.5	0.430
14	OWS	112.0	638.74	-43.0	0.367

The estimates of Table 4-5 should be interpreted with care. As is explained in the Appendix, the CM is modeled in a simple manner. The MDA and STS structures are carefully modeled, together with their internal equipment. In this survey, all equipment remains in the MDA, while in actuality much of the equipment will be transported into the OWS. The AM and OWS geometry models are incomplete. Finally, the self-shielding afforded by a film repository is not included in the computation.

In summary, all dose estimates will decrease by a factor of two to four within film repositories; the MDA and STS estimates will rise as equipment is off-loaded; and the AM and OWS estimates will decrease as additional equipment is included in the computational model.

APPENDIX A

LSVDC4 DESCRIPTION

The three components of the LSVDC4[3] (Lockheed Space Vehicle Dose Calculator - FORTRAN IV) system are the geometry test program, the geometry program, and the dose program. The geometry test program, GEOTST, performs certain logical checks on the geometric data and provides cross-sectional plots of the configuration for visual confirmation of the geometric model. The geometry program, GEOM, processes geometric and material data, prepared by the user, into a form suitable for shielding calculations. The dose program, DOSE, combines geometric data, obtained from the geometry program, and radiation source data and computes the dose at specified detector points.

GEOTST

The geometry test program is an essential adjunct to the geometry program in that it provides computer assistance in checking geometric input data. The fundamental unit of the data is the volume element; the data are read into the program one volume element at a time.

Each volume element is defined by its material composition, density, and bounding surfaces. Five types of volume element boundaries may be used:

- planar surfaces
- ellipsoidal surfaces
- elliptic cylindrical surfaces
- elliptic conical surfaces
- elliptic toroidal surfaces of revolution

A maximum of 25 surfaces, each with unrestricted orientation, may be used to bound a volume element. Each volume element requires the bounding surface data, the number of planar surfaces, the number of quadric plus toroidal surfaces, a material number (1 to 499), the density, and the coordinates of an internal point. The surfaces are specified by the coordinates of three points and zero to three parameters, depending on the type of surface. The coefficients for the algebraic representation of the planar, quadric, and quartic surfaces are computed internally by the geometry program.

A feature termed "embedding" is employed to reduce the number of volume elements required to specify a configuration. Embedding permits volume elements to be located partially or completely within other volume elements. If two or more volume elements compete for a common region of space, dominance is assigned by the order of data input. Thus, a simple box may be specified by six volume elements, one per side, or with the aid of embedding, by two, a void followed by a larger, solid parallelopiped. In the latter case, the contents of the box - if any - must precede the void volume element. Embedding is also a convenient means of incorporating an atmosphere into a complex spacecraft.

Problem set-up time is reduced with the aid of a transformation option. A portion of the configuration may be specified in some convenient coordinate system, then rotated and translated to the correct location. This feature is used extensively in the present study. One example of this option is the use of a transformation to "move" the different camera models from their convenient system to the spacecraft coordinate system. In this way, identical sets of data are used to represent the NRL A camera in the CPSM and in the ATM, the only difference being in the transformations applied.

Computer time is reduced by a factor of three to ten with the aid of a "super region" feature. A super region is a fictious volume element, bounded by two planes and an elliptic cylinder, which contains one or more volume elements. The super region is turned on with the appropriate geometric data and a material number of minus one (-1).

This data set is followed by volume elements completely contained within the super region. The super region is then turned off with a material number of minus two (-2). Super regions may be nested within each other to a level ten deep. In the present study, for example, a super region is placed around the ATM/RACK. Another is nested inside the first around the NRL-B experiment. A third is nested within both around the NRL-B camera. During the geometry search, the program checks to determine whether a vector penetrates a super region. If it misses, the program then skips over volume elements contained within that super region.

Data preparation is eased by using the NAMELIST data input option common to most FORTRAN systems and a procedure that preserves data from the preceding volume elements. This technique permits the user to input only that data which changes from the preceding set and typically reduces the card deck size by a factor of three.

The geometry test program first scans the input data for incorrect formats and characters. Card images containing errors are printed off-line. The program also checks for certain logical errors which would lead to ambiguity in the definition of volume elements. Erroneous volume elements are identified and printed off-line. Finally, it plots cross sections of the configuration as specified by the user. The cross sections are unrestricted in orientation. The grid size of the printer plots is variable to a maximum of 130 by 500. An alpha-numeric character is assigned each volume element appearing on the plot, and a table follows each plot indicating volume element number, density, and material number associated with each character assignment. Exhaustion of the character list, which contains 43 characters, causes a new plot to be started. This geometry test program has proved to be invaluable for verifying and correcting complex geometric data.

GEOM

The purpose of the geometry program is to discover the shielding afforded a detector by a configuration of materials. To realize this purpose, the previously discussed volume elements are constructed and scanned in the following way.

An axially symmetric figure is generated by rotating line segments about the z-axis. A rotated line segment generates a truncated conical or cylindrical shell. Each shell is approximated by six equal planar facets. Each facet is subdivided into regions until the solid angle subtended by each region at a detector is less than the input solid angle criterion for that facet. This feature permits critical shield areas to be examined more closely than others.

A vector array associated with each detector is then generated. Each vector joins the detector to the centroid of a region. Those segments of each vector which lie within volume elements are found and arranged in order from detector outward. The penetration lengths, material numbers, solid angle, and vector direction cosines are put on tape for use by the dose program.

DOSE

The task of the dose program is to compute primary proton and related secondary dose, alpha and related secondary dose, and electron and bremsstrahlung dose at detector points associated with the geometric configuration. The location of the detectors with respect to the configuration and its component volume elements is in no manner restricted.

The dose program approximates the appropriate proton spectrum, differential in energy, with from one to 100 power law representations over the energy range of interest. The source and geometric data are applied to an attenuation method, which is suggested by M. O. Burrell[2]. The validity of the proton dose calculation has been tested by comparing the results to those of the Lockheed Proton Penetration Code in spherical shell shield geometry for isotropic flux. Several spectra, materials, and material combinations have been examined.

The alpha dose calculation is similar in method to the proton dose calculation. The alpha-induced secondary dose estimates are less reliable than proton-induced secondary estimates due to a scarcity of experimental and theoretical data.

The electron dose calculation converts material thicknesses to their aluminum equivalent on an electron density basis and computes electron penetration number flux according to a method suggested by Mar[7]. An energy spectrum is assigned to the number flux by an empirical technique and an energy deposition dose is calculated.

The bremsstrahlung calculation combines electron flux data throughout the shield with bremsstrahlung cross sections recommended by Koch and Motz[5] and a point kernel attenuation technique[3] to estimate bremsstrahlung dose. The electron fluxes are based on equivalent aluminum shields; however, bremsstrahlung production is based on actual materials present.

The DOSE program contains two options which facilitate certain types of investigations. The first option permits variation of densities according to material number. This feature permits shield thickness parameter studies to be made without rerunning the GEOM program. The second option permits calculation of the dose entering within user-specified solid angle regions and comparison with average dose per steradian. This feature may be used to check for radiation streaming and to generate data for shield shaping optimization.

APPENDIX B

CLUSTER CONFIGURATION

Two AAP configurations are examined in the present study. The first, Figure B-1, is the AAP 3/4 mission. The AAP 3 CSM is docked in the axial MDA port, and the AAP 4 LM-ATM/RACK is docked in radial port I for 56 days. The second configuration, Figure B-2, is for the AAP 2 mission. It is identical to the first configuration except that the LM-ATM/RACK is not present. The primary purpose of this study is to assess the radiation hazards to ATM film; the greatest emphasis is placed on simulating the ATM geometry. Secondary emphasis is placed on ATM film storage locations and still less emphasis on the remainder of the cluster. The cluster geometry model is composed of 1400 volume elements.

Each module of the AAP cluster is discussed briefly to indicate the level of detail covered in that module. Components which are treated in insufficient detail are noted.

ATM/RACK

The ATM/RACK configuration is illustrated in Figures B-3 and B-4. A weight is computed for each volume element in the mathematical model of the ATM and is checked against a detailed weight statement[8]. The ATM model "weighs" 15171.2 pounds compared to a weight statement total of 18504.0 pounds. Thus, 82.0 percent of the actual mass is included in the model.

A large part of the missing weight is structure. Approximately 900 pounds of the 2102.6 pounds of structure is not modeled. A portion of this omission is due to lack of detailed blueprints and a portion is due to the difficulty of simulating a large number of small parts such as rivets, splice plates, and stiffeners. Approximately half the missing 900 pounds could be modeled if the necessary information were available.

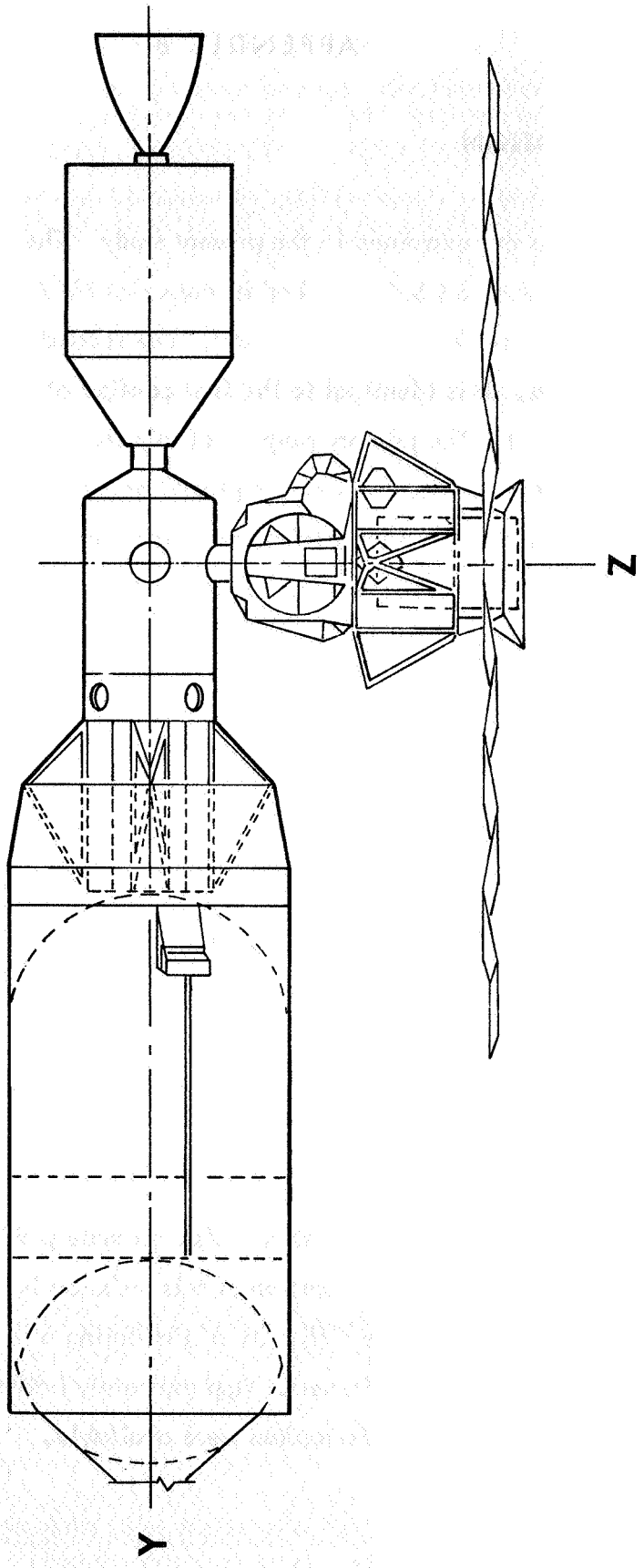

FIGURE B-1 AAP 3/4 CLUSTER CONFIGURATION

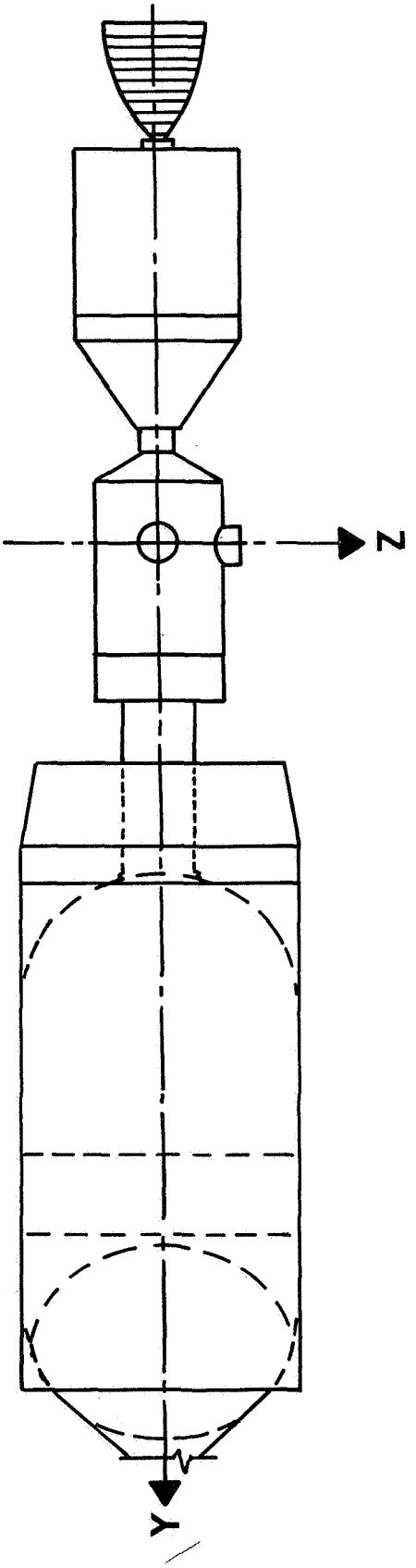

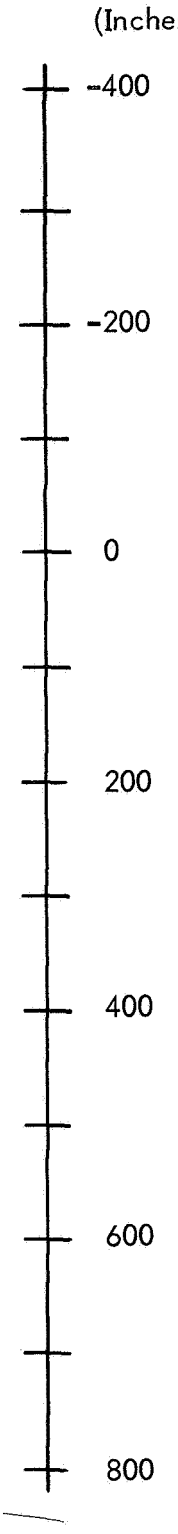

FIGURE B-2 AAP-2 CLUSTER CONFIGURATION

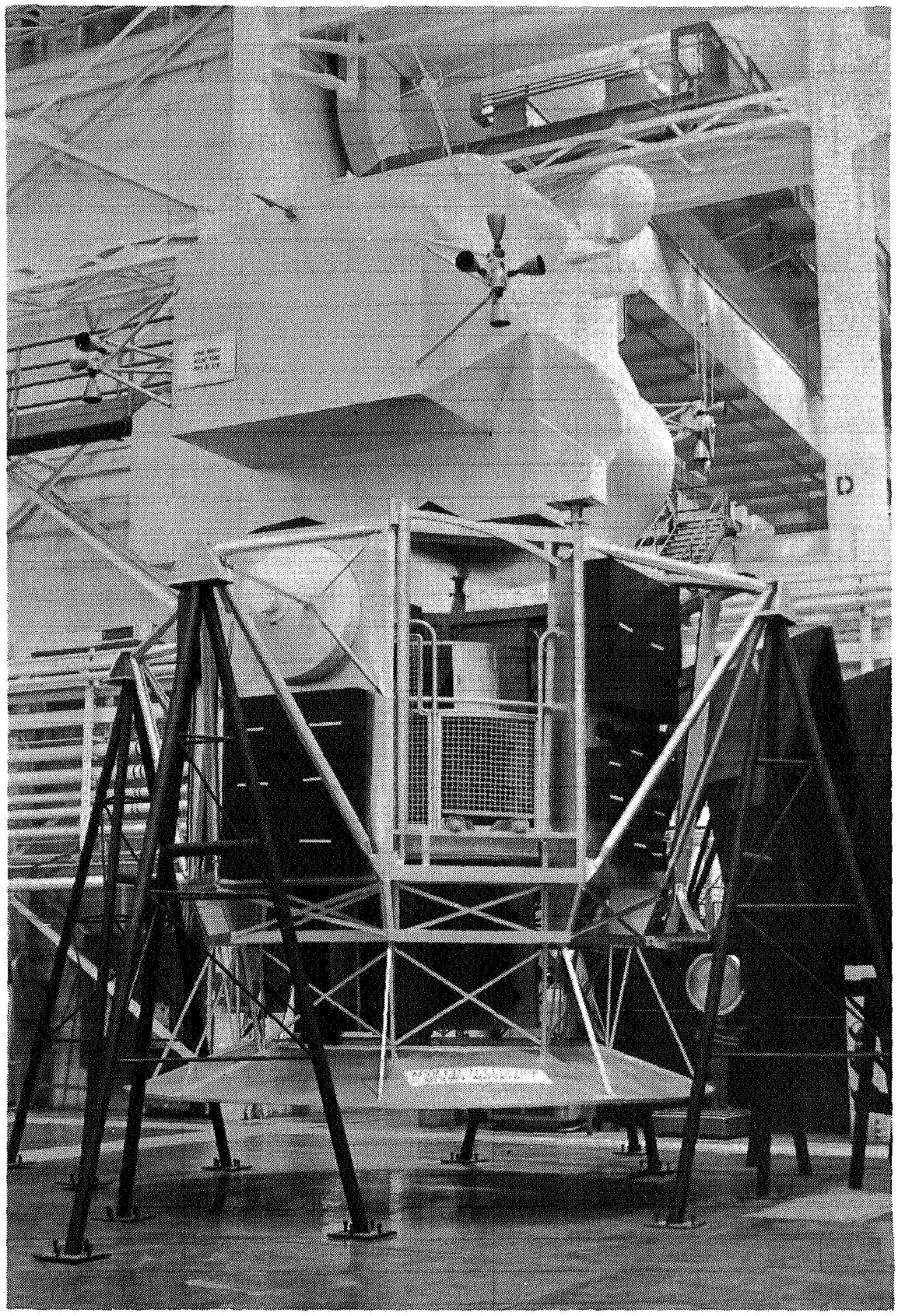

B-3 LM ATM/RACK MOCKUP

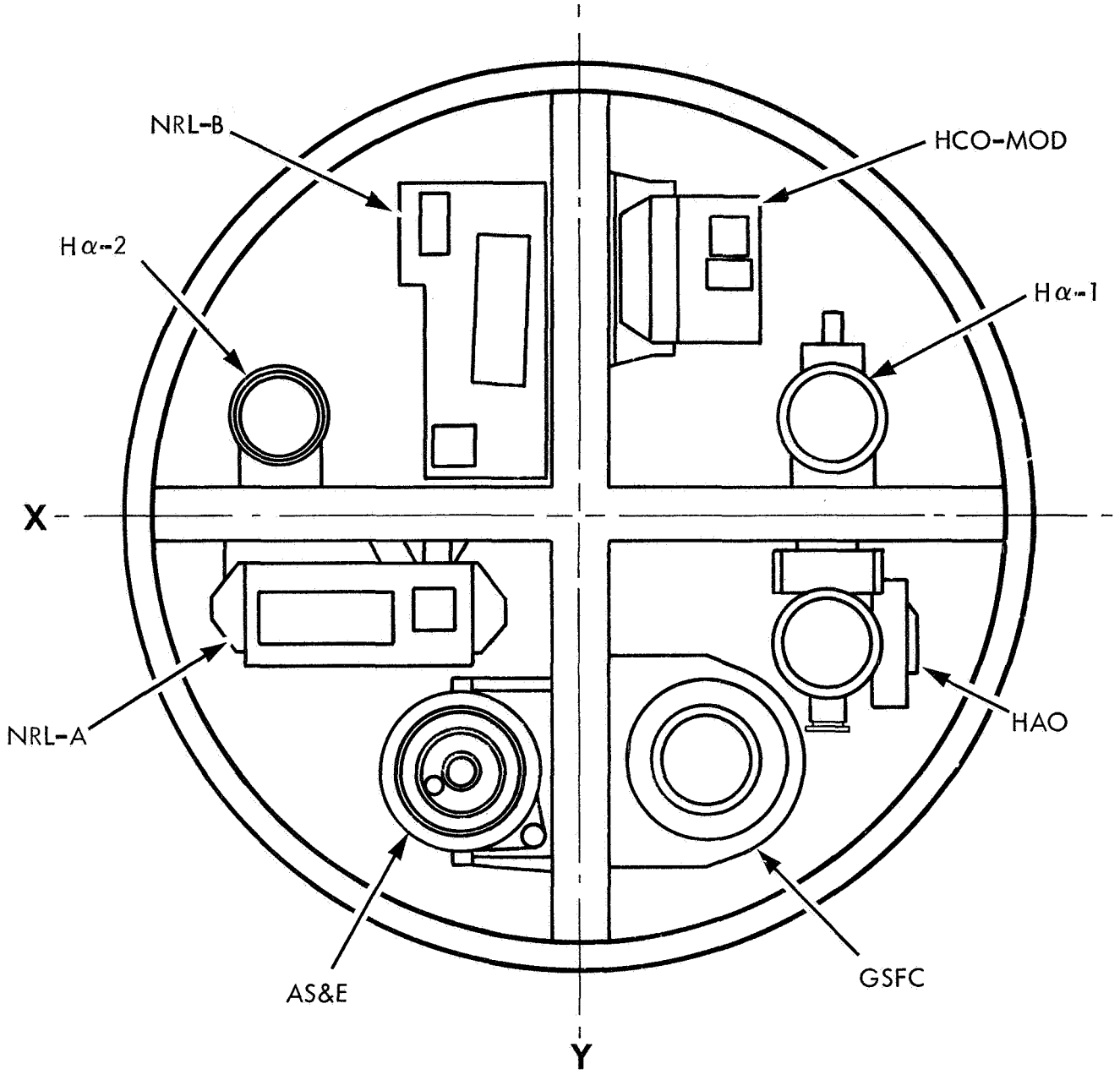

FIGURE B-4 ATM CANISTER (SUN END)

Equipment mounts on the rack totalling 267.1 pounds are omitted. These items offer little shielding effectiveness because they are adjacent to massive components. Approximately 100 pounds of important (from a shielding standpoint) miscellaneous equipment is not modeled due to lack of information. It is particularly unfortunate that the 64.5 pound LM end work station does not appear on any of the blueprints scanned, because this component is in a lightly shielded region.

Nearly all the electronics boxes mounted on the rack comprising the measuring system, rf system, telemetry system, pointing control subsystem, and the electrical system are modeled. Each box is given the proper dimensions and location, and the contents are homogenized. However, 330 pounds of cables and wiring on the rack are omitted. It is not feasible to simulate much of the dispersed wiring. Because the homogenization of boxes leads to optimistic shielding estimates, while omission of cabling leads to conservative shielding estimates, these two factors will compensate each other to some degree.

Only 585.4 pounds of the 922.9 pound gimbal system is modeled. The lost weight is not important for shielding purposes because it is concentrated in a small region already shielded by other massive components.

The thermal control insulation on the rack, totaling 162 pounds, is omitted except for 17.2 pounds near the astronaut work station, a lightly shielded area. Most of the remainder of this insulation is not effective for shielding purposes because it covers massive components. Additional configuration information is necessary to incorporate the missing covers.

The ATM solar array model appears to be adequate from a standpoint of mass (over 4000 pounds) and dimensions. The antenna panels (48 pounds) are not included because these are unimportant from solid angle considerations.

The ATM spar is composed of two aluminum plates, each 120" x 74" x 1", mounted in a cruciform shape within the canister. The ATM telescopes are mounted on the spar. This component offers severe modeling difficulties because it contains approximately 1000 circu-

lar holes drilled to lighten the spar in those areas where telescope mount brackets are not attached. In the present study, the number of volume elements required to simulate the spar is reduced from approximately 1000 to 156 by criss-crossing aluminum laths, leaving rectangular holes. The spar model has the correct weight, 1224.5 pounds.

The top and bottom spar rings, 57.1 pounds each, and the girth ring, 193.6 pounds, are modeled. However, 412.8 pounds of fittings, plates, brackets, and launch locks are omitted due to lack of data, as are 20 pounds of half-micron filter and 100 pounds of ballast.

The sun end experiment door assemblies contain complicated mechanisms which are difficult to model. Fortunately, these assemblies subtend a small solid angle from most of the cameras. They are, therefore, approximated by ten circular discs with appropriate size and location. The door model weighs a total of 160 pounds compared to an actual 206.7 pounds.

Eighteen electronic boxes and ATM rate gyros are accurately positioned on the canister and spar, totaling 234.5 pounds. Canister cables, totaling 130 pounds are omitted due to their dispersed locations. This omission should not be serious because they are generally attached to massive components, such as the spar, and offer little additional shielding.

The thermal control system for the canister includes the canister walls, radiator, and insulation, plus the spar insulation. A number of small pumps, manifolds, etc., are omitted due to lack of detailed information. The modeled weight is 604.7 pounds, or 78.1 percent of the 774.1 pounds allotted to the canister thermal control system.

Eight telescope experiments are located on the ATM spar, six requiring cameras and film. The experiments are listed in Table B-1, together with their actual and modeled weights, including camera, vidicon, etc. The camera weights are also stated due to their large influence on computed dose. Camera geometry models are shown in Figures B-5 through B-7.

The first experiment in Table B-1, the HAO S052 White Light Coronograph, is the poorest modeled telescope from a weight standpoint, though a relatively large amount of detail is

TABLE B-1 ATM EXPERIMENT WEIGHTS

Experiment	Experiment Weight	Model Weight	Camera Weight	Model Weight
HAO SO 52	330.0	163.0	22.0[1]	11.3
AS&E SO 54	267.0	213.5	38.0[2]	24.4
GSFC SO 56	354.0	298.6	12.5[3]	11.3
NRL-A SO 82A	293.5	266.6	42.0	33.3
NRL-B SO 82B	367.5	353.9	40.0	33.3
H-ALPHA 1 SO 55	185.0	163.4	12.5[3]	11.3
H-ALPHA 2	110.0	117.5	--	--
HCO-A MOD	335.0	335.0	--	--

Notes:

1. Includes handle and lens face cover - 3 lb.
2. Includes Image Intensifier Assembly - 4 lb.
3. Includes handle - 1.5 lb.

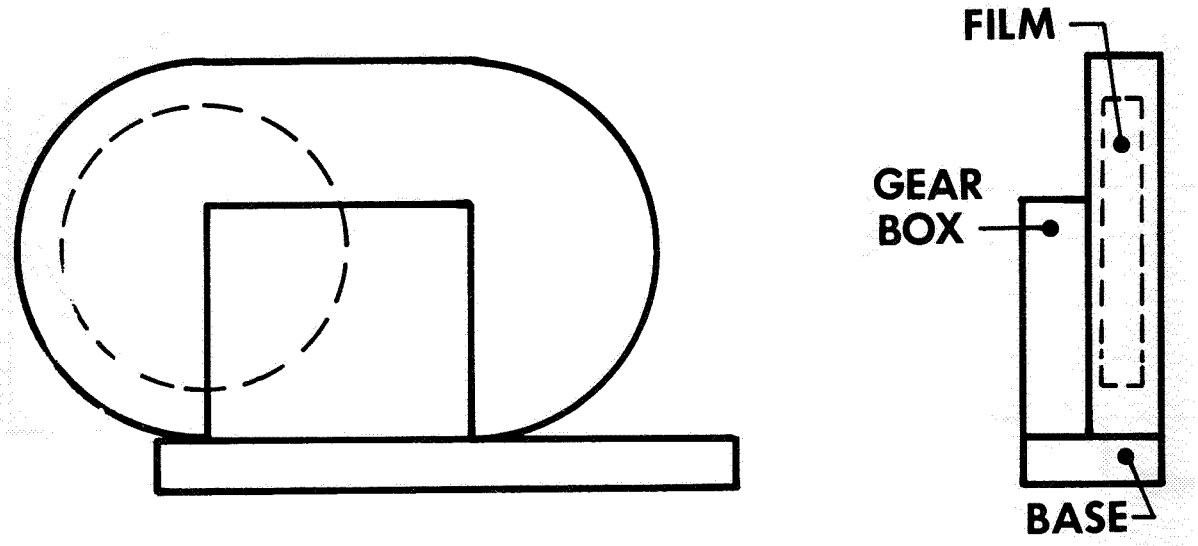

FIGURE B-5 GSFC & H-ALPHA CAMERA MODEL (ALSO HAO)

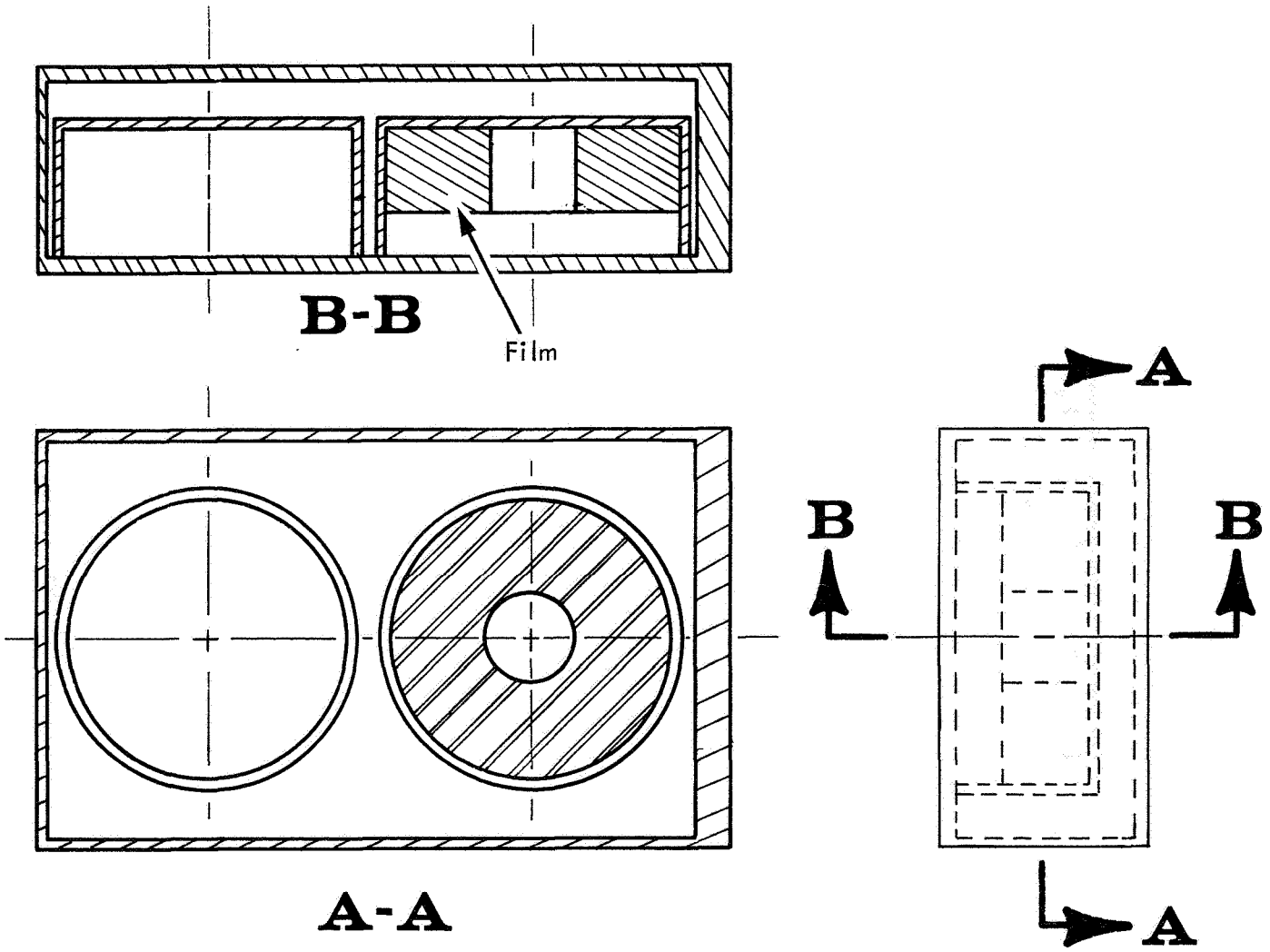

FIGURE B-6 AS&E CAMERA

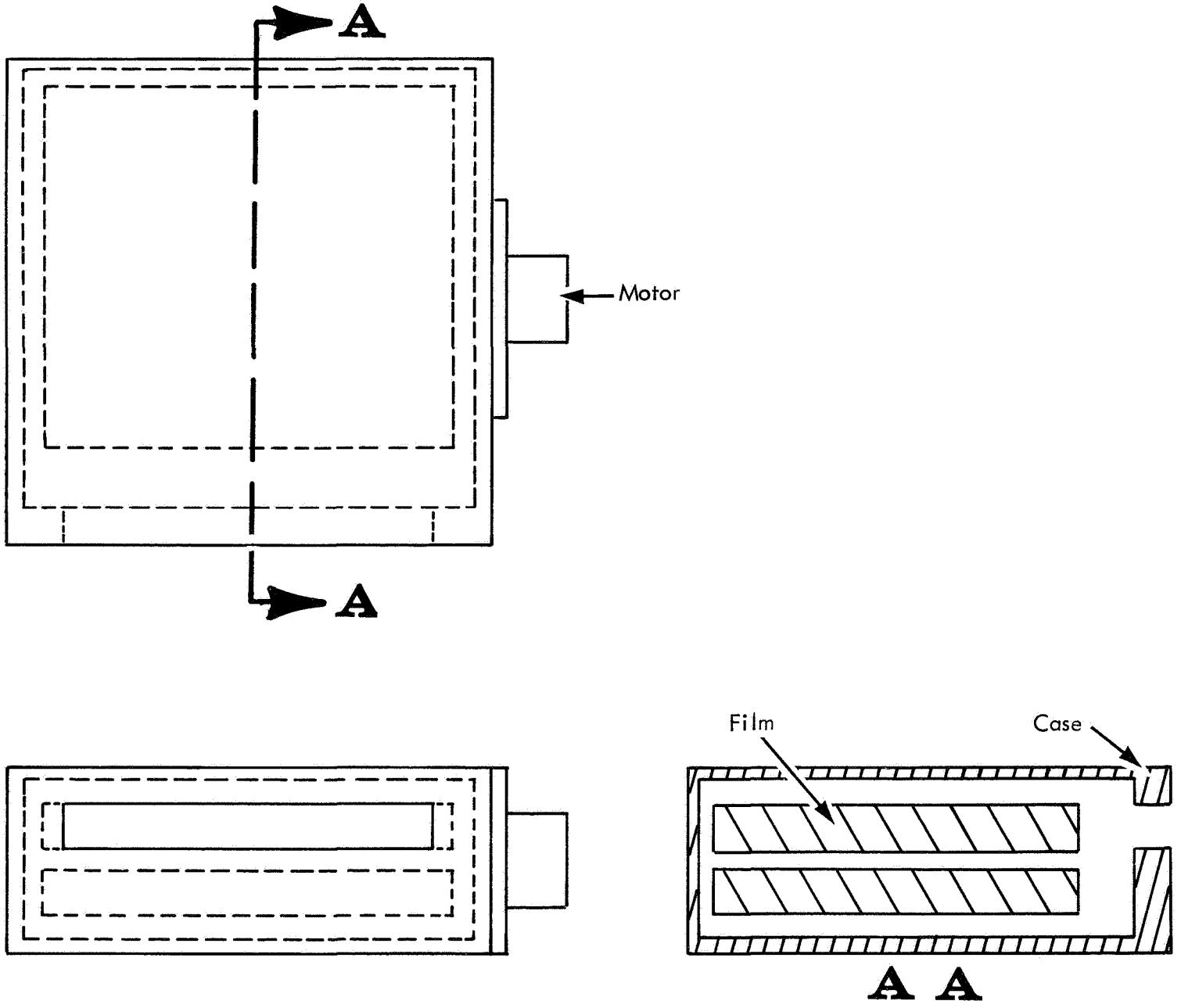

FIGURE B-7 NRL A&B CAMERA

LM and CPSM

The LM vehicle, Figure B-3, is modeled in a simple manner with few volume elements and several blocks of homogenized equipment. The skin mass thickness is increased slightly to partially account for structure and micrometeoroid bumper. No effort was made to improve the LM model during the present study; instead it is recommended that a LM model[6] prepared for MSC by another contractor be adapted to the LSVDC4 system.

The Crew Provisions and Stowage Module (CPSM) is modeled adequately and placed around the LM docking tunnel, Figure B-8. Fourteen small components plus the radiator are placed outside the CPSM wall. Eighteen cameras and two empty storage cassettes for the NRL cameras on the ATM are situated in the CPSM. Unique material numbers are assigned to each set of cameras so that they may be removed during dose program runs. This treatment permits calculation of dose rate changes to the remaining cameras as cameras are removed during EVA for use on the ATM.

APOLLO CSM

The Apollo Command and Service Modules (CSM) are modeled in a fairly simple manner with primary emphasis upon correct skin mass thicknesses. The SM contains an engine, nozzle, fuel tanks and gas tanks. The tanks are assumed to be half full of homogenized fluid. The CM contains three seats, six cameras, and four equipment bays with homogenized contents.

MDA and STS

The Multiple Docking Adapter (MDA) and Structural Transition Section (STS) shown in Figures B-9 through B-12 are modeled in adequate detail. The MDA possesses one axial docking port for the CM and two radial docking ports suitable for the LM. The MDA is considered in four segments; a conical section, an upper cylinder, a port cylinder, and a lower cylinder. The skin, lands, and braces are represented in each segment. Insulation

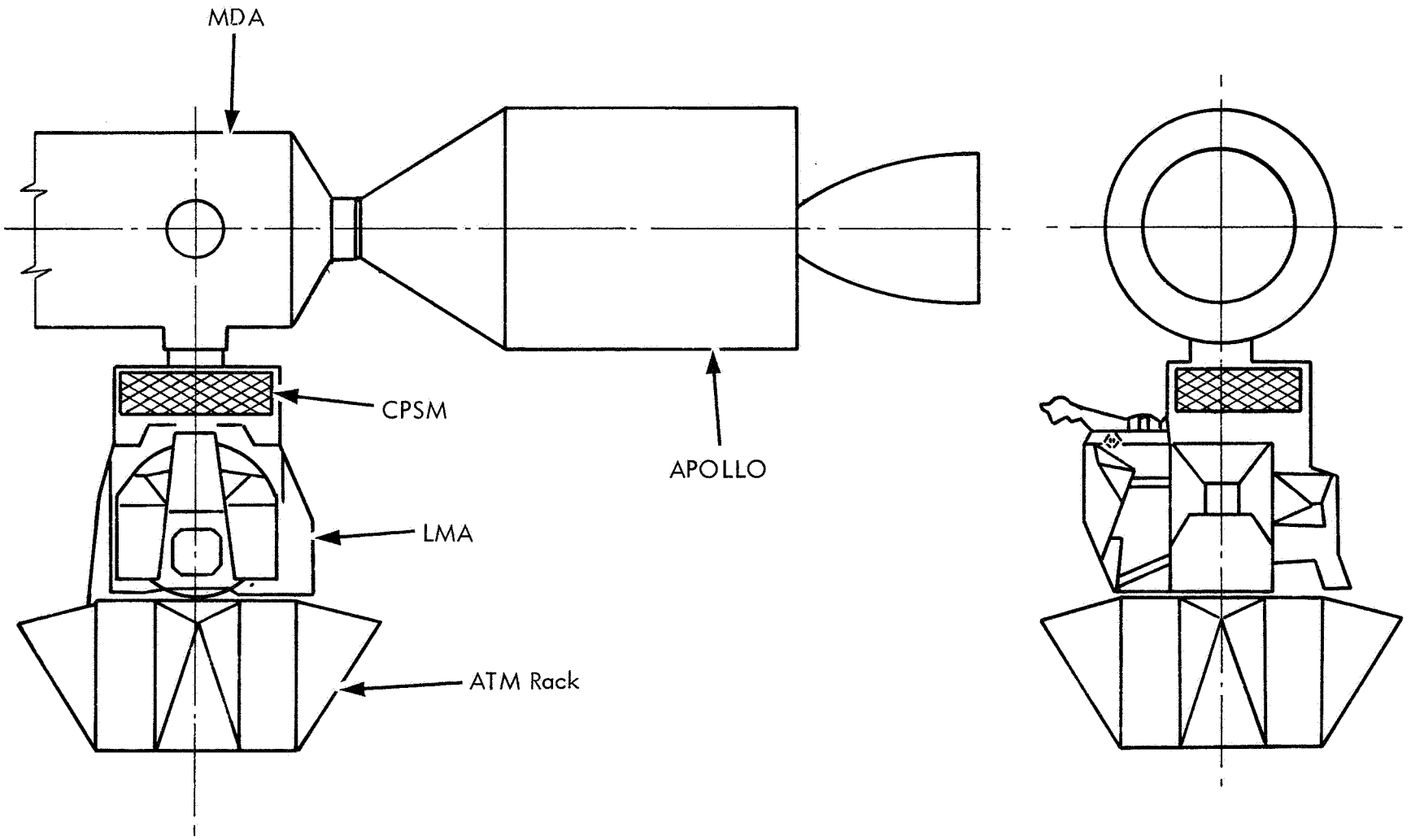

FIGURE B-8 CPSM LOCATION

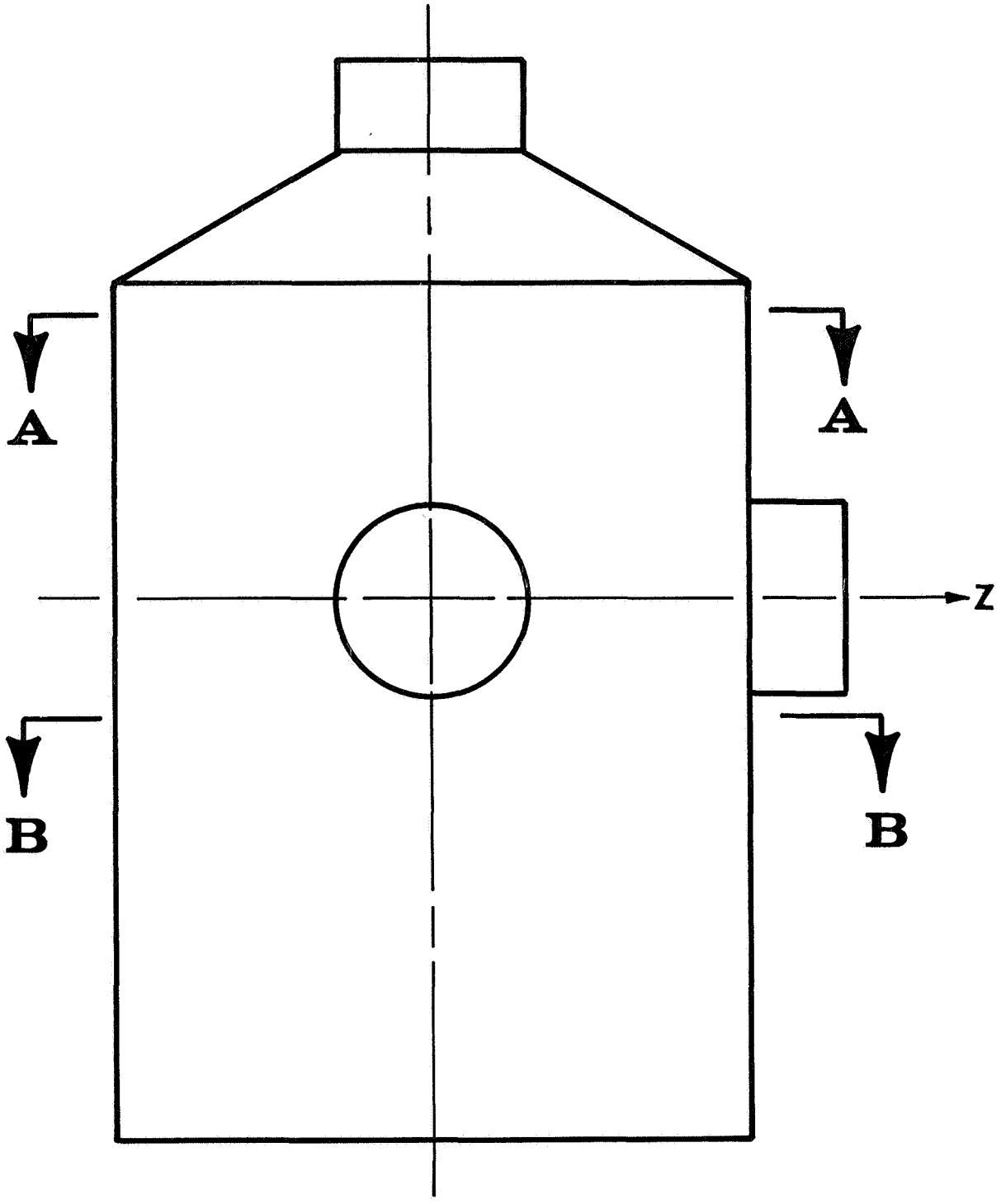

FIGURE B-9 MDA CONFIGURATION

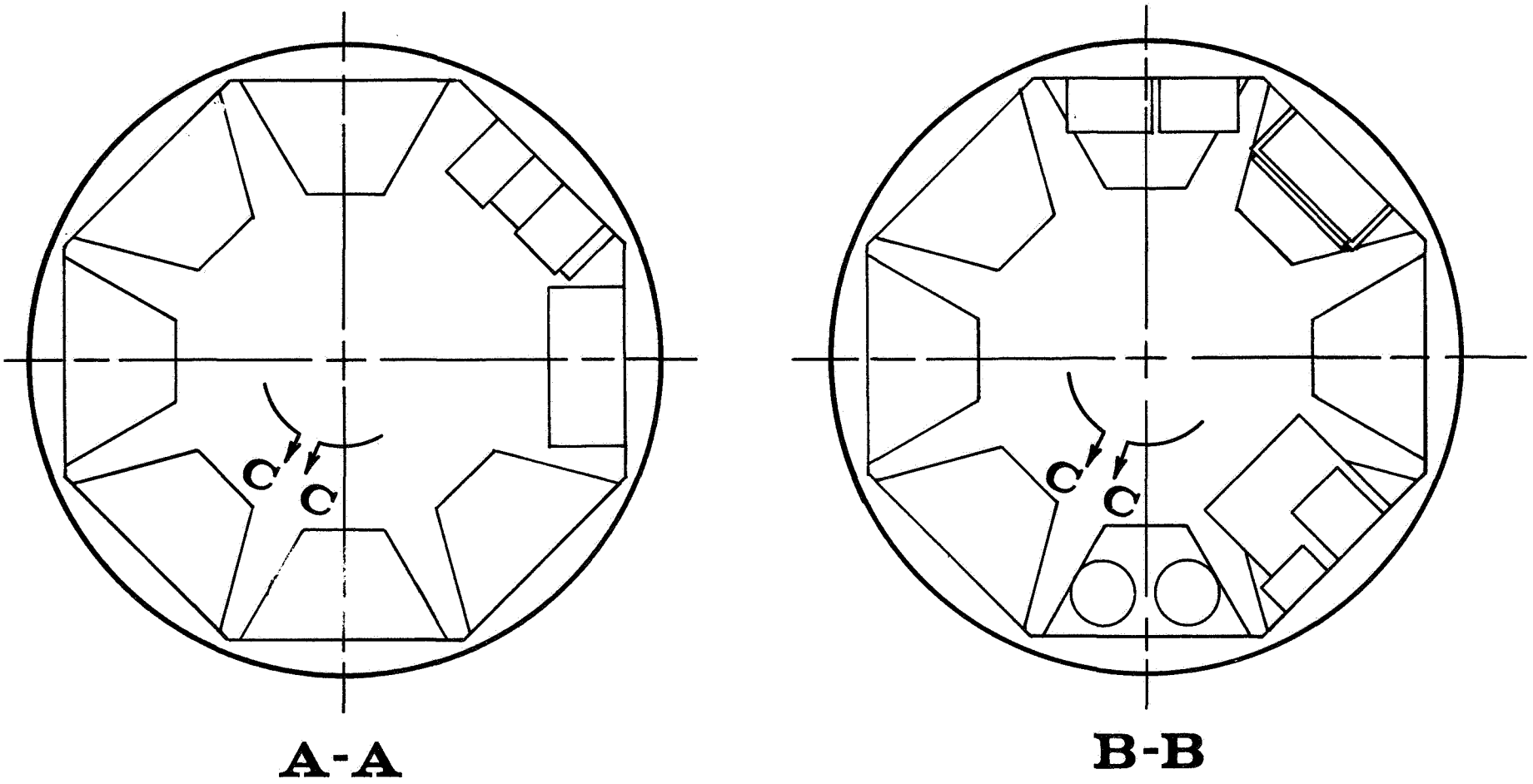

FIGURE B-10 TYPICAL MDA ARRANGEMENT

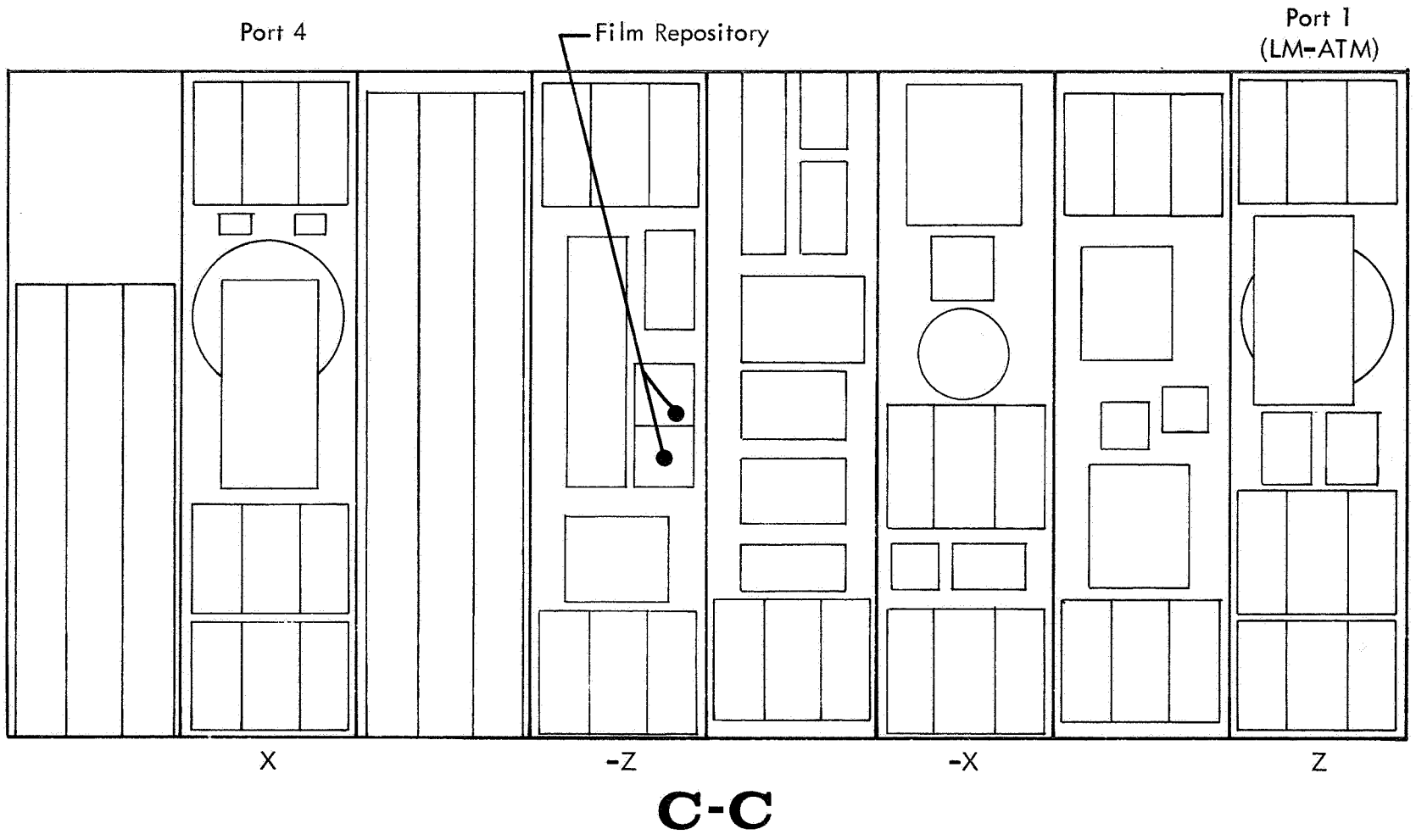

FIGURE B-11 MDA INBOARD PROFILE - SPACE ENVELOPE LAYOUT

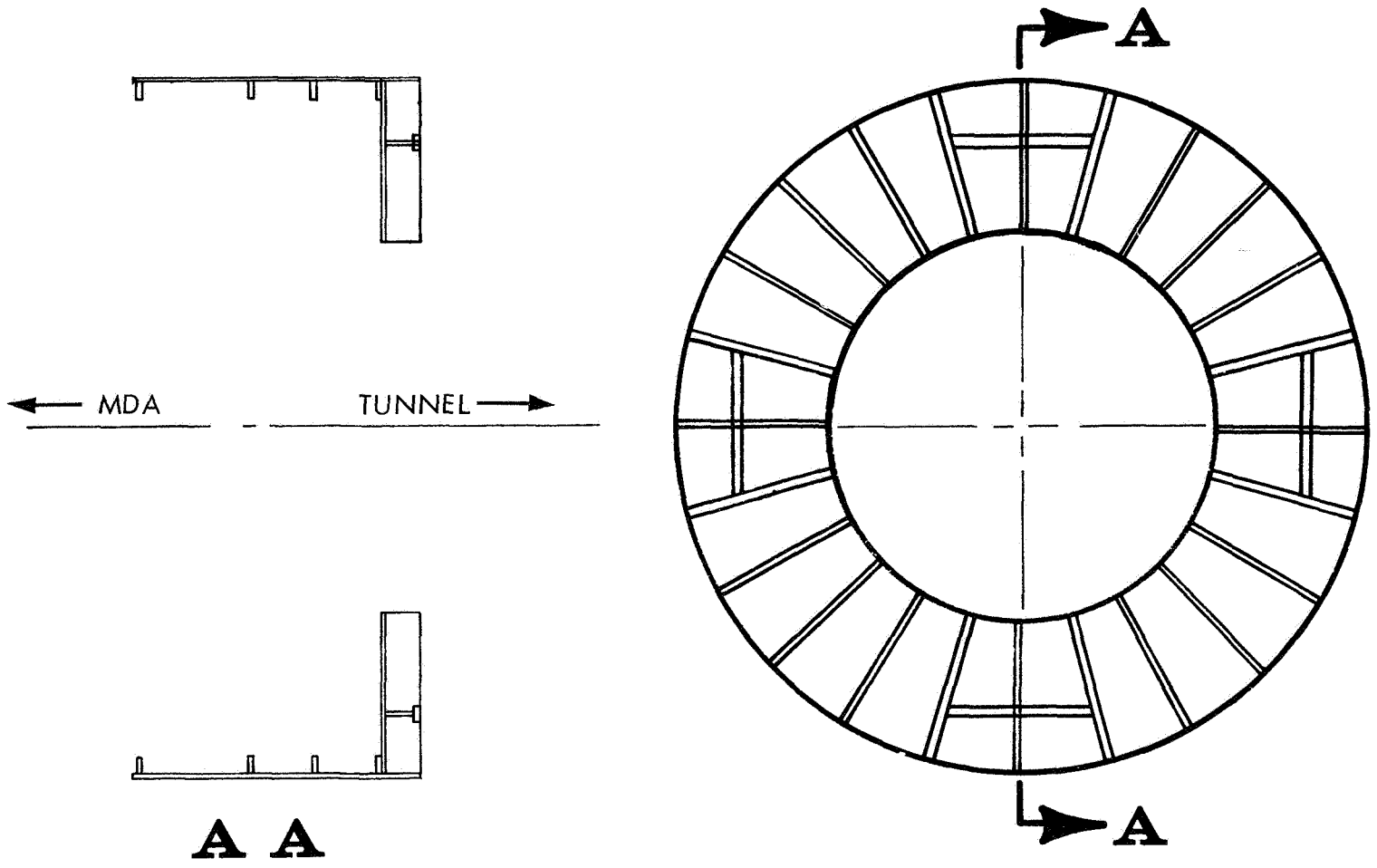

FIGURE B-12 STS ASSEMBLY

considered. Thirty-six volume elements are used in the telescope proper and ten in the camera. Part of the weight underestimate is due to omission of ribs on the optical housing (5-10 pounds), and part is due to omission of experiment mounts which add little shielding because they are shadowed by the optical bench and spar. However, the majority of telescope weight discrepancy is probably due to use of very preliminary information with outdated thickness dimensions. The low camera model weight results from use of an SO 56 camera instead of an HAO SO 52 camera for which no data were available. The HAO telescope film hazard should be re-examined when additional data are available.

The AS&E SO 54 telescope is fairly well modeled though further detail could be accommodated in the electronics, supports, and camera interface. The camera itself is fairly well modeled in wall thicknesses, film, and supply and take-up cassettes. Additional detail is desirable in the camera mechanism. The four pound image intensifier assembly is not included.

The next four telescopes, GSFC SO 56 through H-alpha 1 SO 55, are modeled in adequate detail. The SO 56 and SO 55 cameras (identical) are well modeled except for omission of the handle. The NRL cameras are too light, probably due to omission of part of the mechanism for which no details were available. An attempt was made to account for most of the mechanism with homogeneous volume elements.

The H-Alpha 2 telescope model is approximately seven percent too heavy. No reason is known for this discrepancy, but it should not appreciably affect film degradation estimates.

The HCO-A (Modified) experiment model is over-simplified. It consists of a small box running half the length of the telescope representing electronics, plus a box representing the remainder of the telescope. The electronics box density is arbitrarily set to twice the telescope density and both are adjusted to yield the correct weight. The outside dimensions of each box are approximately correct.

and radiators are included. The inside walls of the MDA are lined with 41 boxes, many of which have trapezoidal cross sections, containing equipment and experiments.

The STS assembly is modeled with skin, insulation, and radiator combined. Four structure rings and the pressure bulkhead are included. The skin is strengthened with 48 stringers. Forty truss attachments, fittings, and splices are positioned on the bulkhead.

AM

The Airlock Module, AM, is modeled in a simple manner. The model includes the airlock tunnel skin, the bellows connection to the SIV B, several battery packs, and 12 gas tanks. The AM model weighs 1878.8 pounds compared to an actual weight of approximately 7000 pounds.

OWS

The Saturn SIV B, converted into an Orbital Work Shop (OWS), is also modeled in a simple manner. It consists of a cylindrical tank with hemispherical ends. The tank wall protrudes over a part of the airlock module as shown in Figure B-2. A hemispherical wall separates the LH_2 tank from the LOX tank. The nozzle is represented by a conical shell volume element. Solar cell arrays are placed outside the cylindrical tank.

APPENDIX C

RADIATION DEGRADATION OF PHOTOGRAPHIC FILM

The dose computations of Section 4 are given in terms of physical dose (rads-air), while the parameter of interest in determining film damage is radiation fogging density. A relationship between physical dose and fogging density has been determined for several films of potential interest to ATM experimenters.

Each film type has been subjected to proton beams of 10, 17.6, 50, 90, and 120 MeV at the MIT and ORNL proton accelerators by MSFC and Langley personnel[1]. The data presented herein are based upon film development and analyses performed at Kodak by K. E. Huff and H. M. Cleare[4], and upon radiation transport analysis by J. W. Watts[10] of MSFC.

Figures C-1 - C-5 illustrate radiation fogging density versus dose at five shield thicknesses for the proton spectrum of Table 3-1. For a given dose, the density generally increases with shield thickness. This effect is due to spectral hardening combined with increasing film sensitivity to increasing energy protons at a given dose. Thus, radiation fogging density depends on the radiation spectrum, effective shield thickness, and the film type. Three film types currently proposed for ATM experiments are included in the data, as well as two faster, more radiation sensitive types (103-0 and Plus-X).

The ATM film fogging densities given in Section 4 are derived by combining the film degradation data with effective shield thickness computations for the CPSM, ATM, and CM. A special program was written to compute the effective thickness, weighting by solid angle and dose rate for each vector which scans the configuration. These effective thicknesses (for the selected detector locations) range from 8 to 14 gm/cm^2 in the CPSM; from 8 to 20 gm/cm^2 in the ATM; and from 28 to 36 gm/cm^2 in the CM.

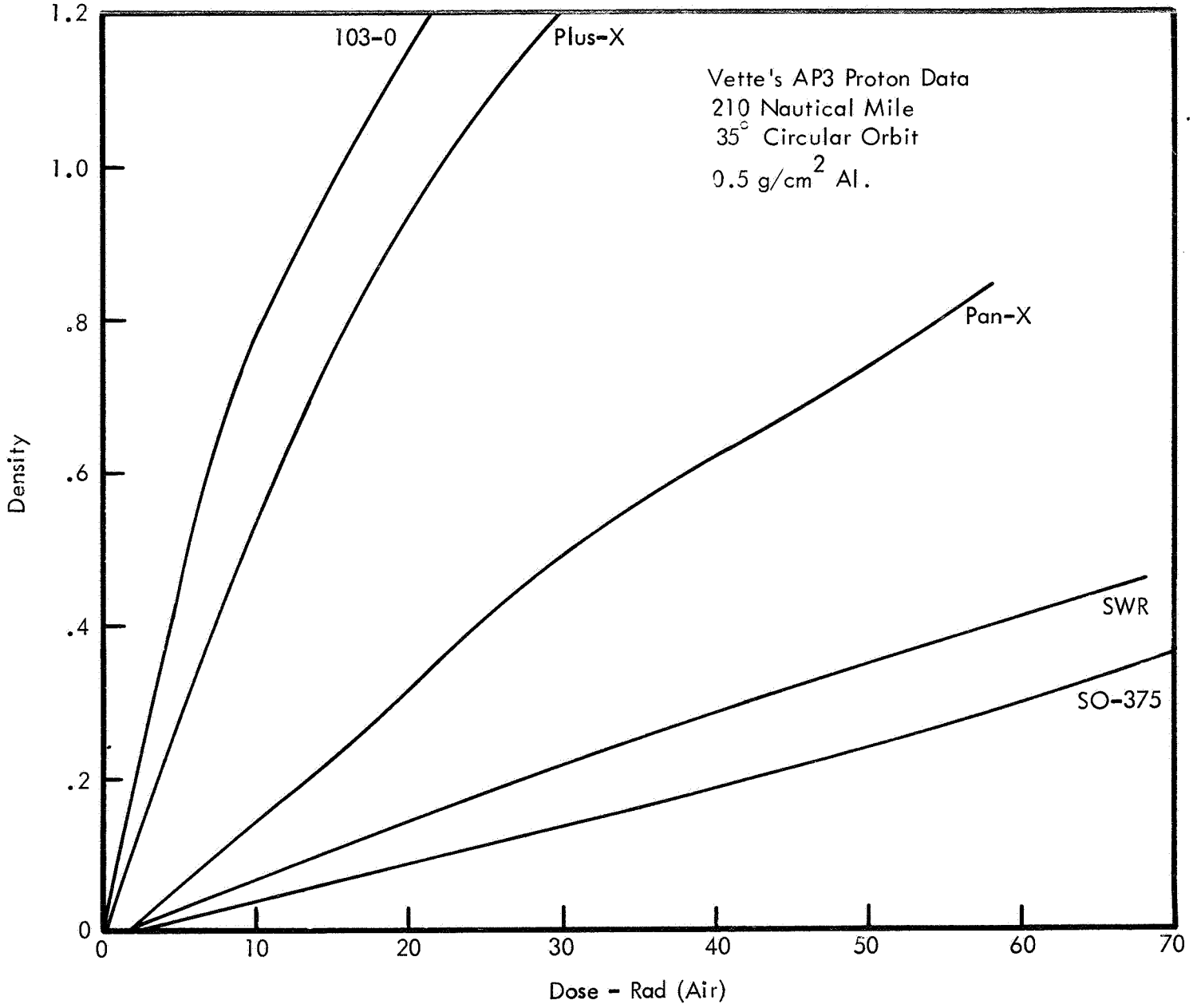

FIGURE C-1 FILM FOGGING DENSITY VS. DOSE

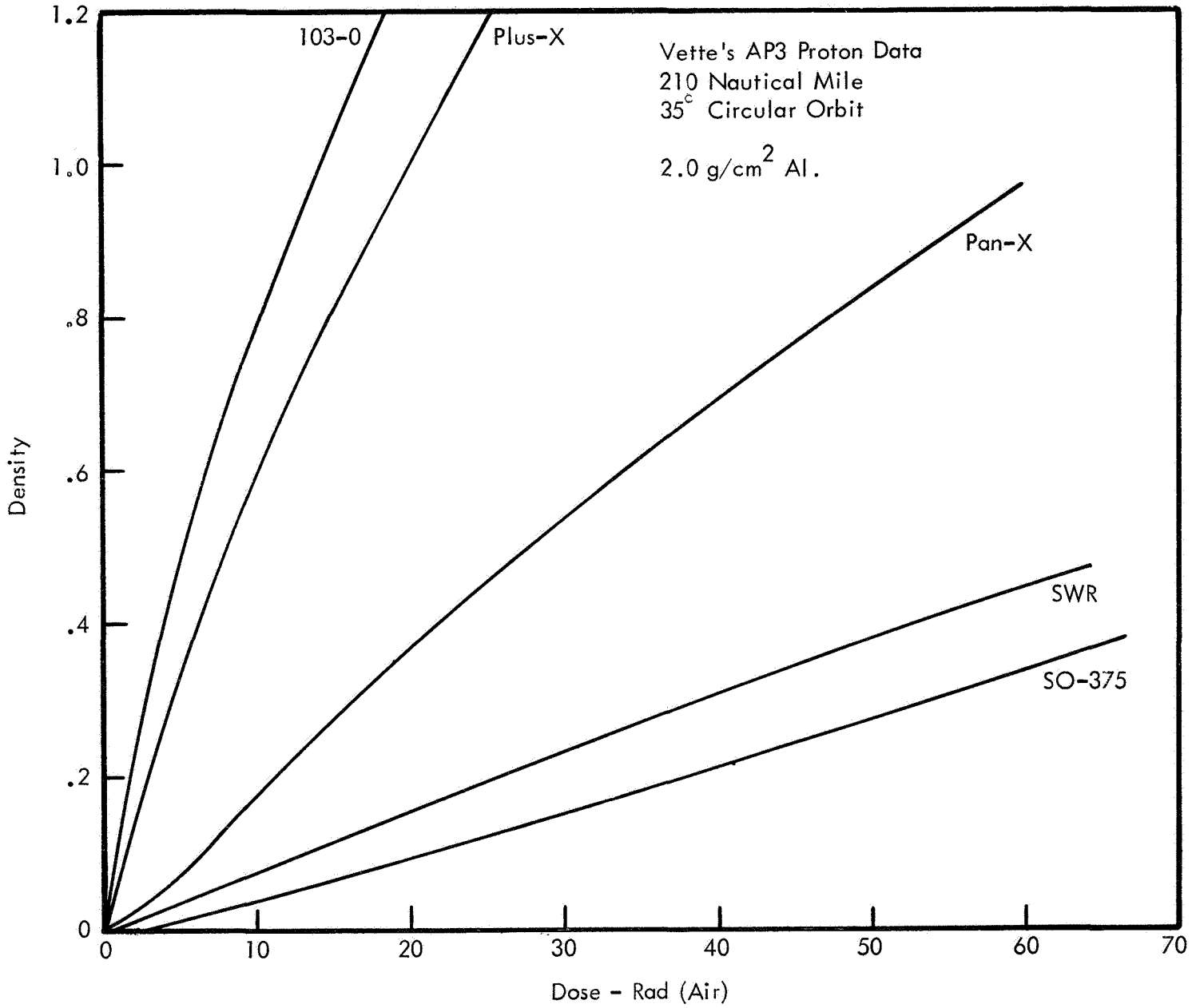

FIGURE C-2 FILM FOGGING DENSITY VS. DOSE

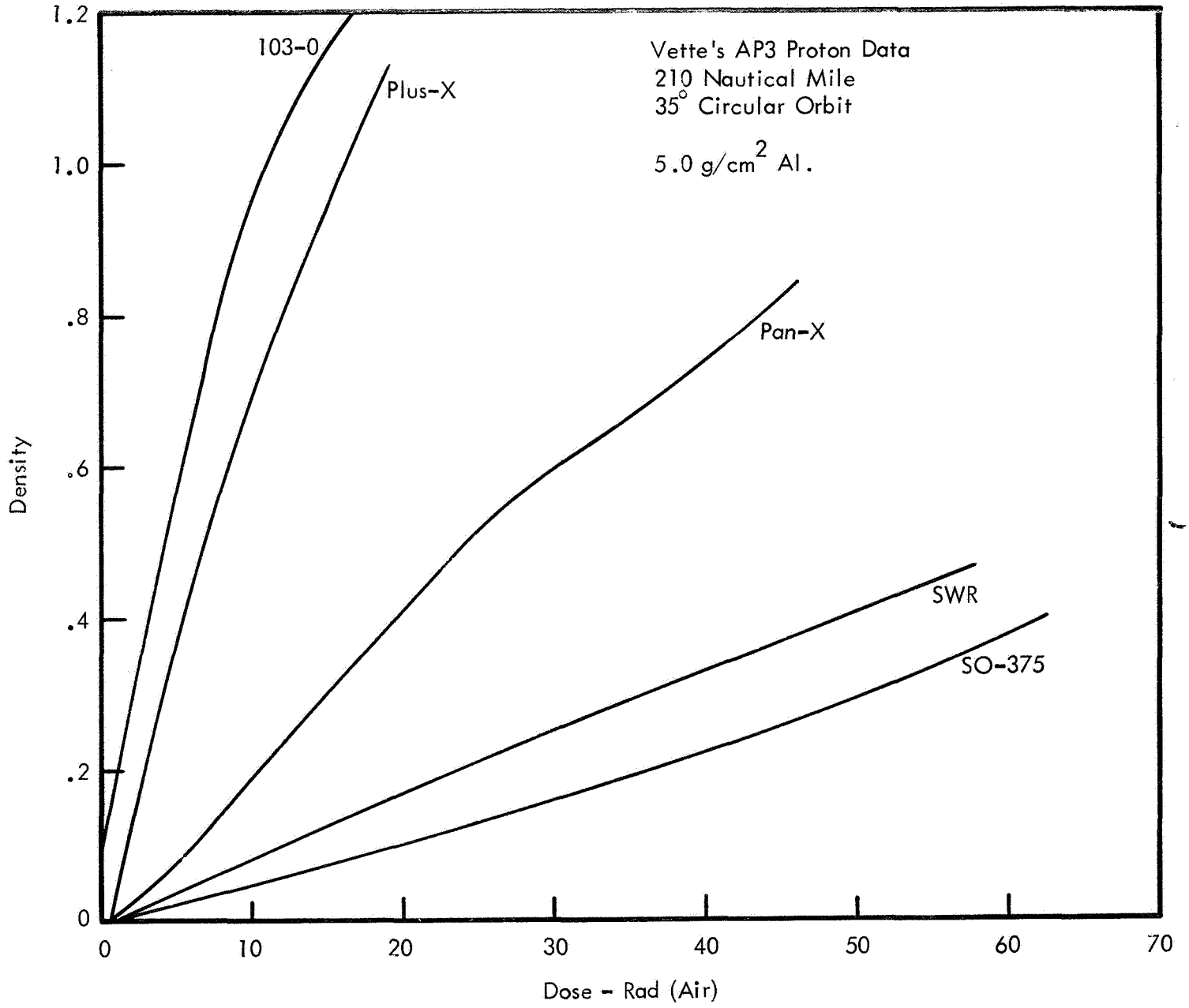

FIGURE C-3 FILM FOGGING DENSITY VS. DOSE

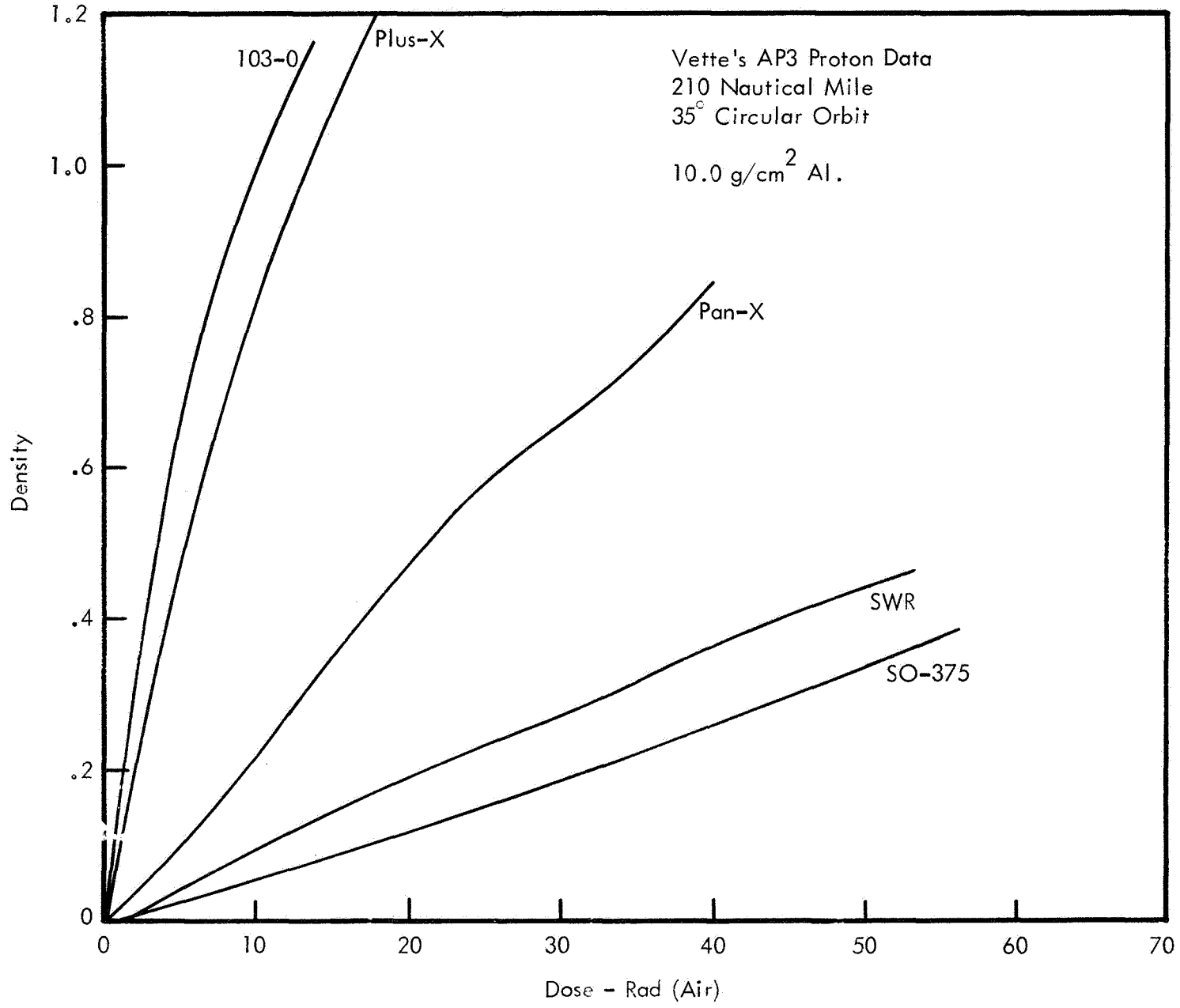

FIGURE C-4 FILM FOGGING DENSITY VS. DOSE

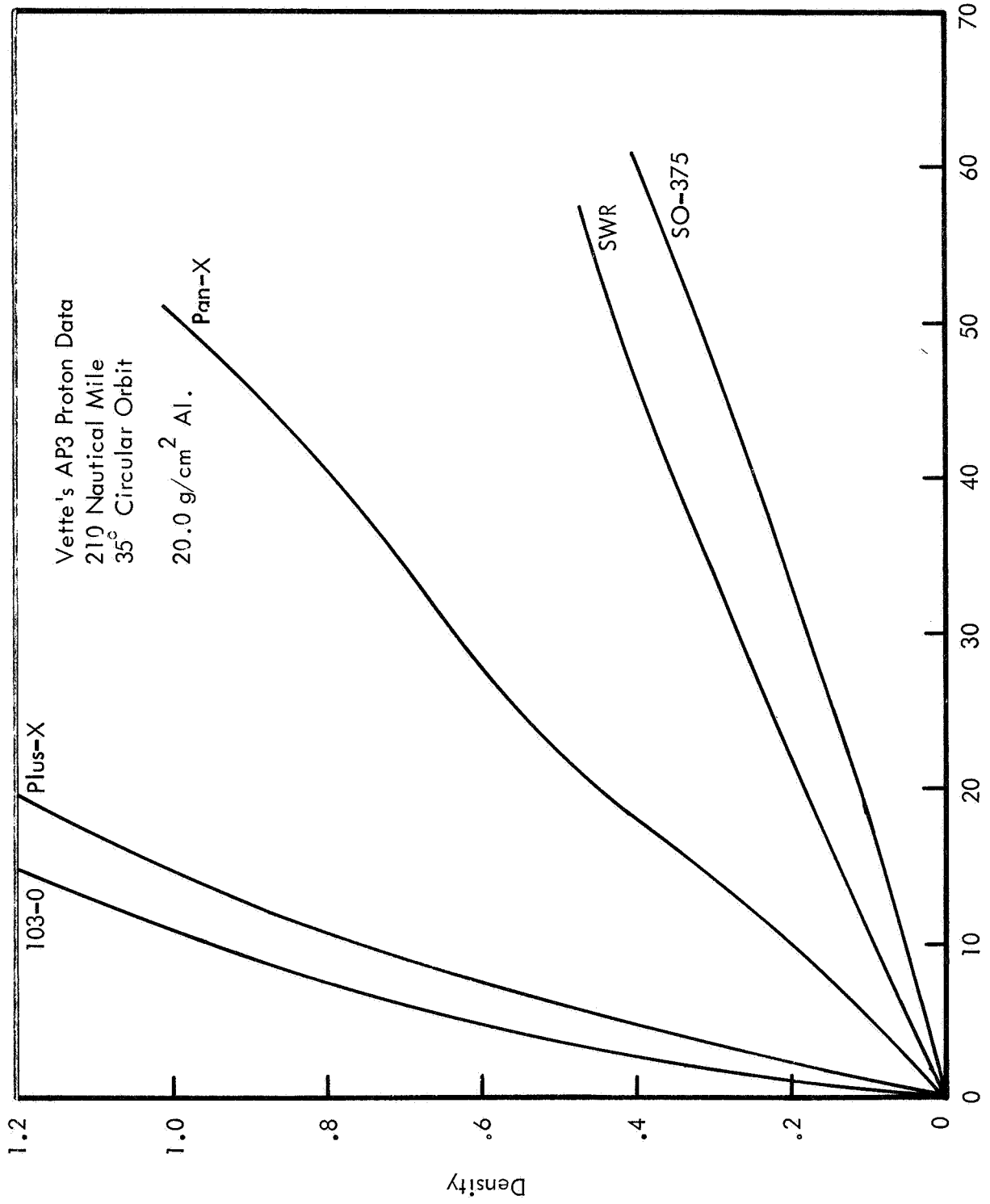

FIGURE C-5 FILM FOGGING DENSITY VS. DOSE

REFERENCES

[1] Breazeale, W. L., Potter, R. A.: Experimental Investigations of Radiation Effects on ATM Photographic Film, MSFC-NASA Working Paper, 1967.

[2] Burrell, M. O.: The Calculation of Proton Penetration and Dose Rates, Second Symposium on Protection Against Radiations in Space, Gatlinberg, Tennessee, October 12 - 14, 1964; NASA SP-71, p. 493, 1965.

[3] Hill, C. W.; Ritchie, W. B.; Simpson, K. M., Jr.: Data Compilation and Evaluation of Space Shielding Problems,
Volume I - Range and Stopping Power Data,
Volume II - Dose Calculations in Space Vehicles,
Volume III - Radiation Hazards in Space,
Volume IV - LSVDC4 Program System,
ER 7777, Lockheed-Georgia Company, Marietta, Georgia, 1965 - 1967.

[4] Huff, K. E.; Cleare, H. M.: Private Communication.

[5] Koch, H. W.; Motz, J. W.: Bremsstrahlung Cross Section Formulas and Related Data, Rev. Mod. Phys. 31, 920, 1959.

[6] Liley, B.; Hamilton, S. C., Fletcher, J. D.: Numerical Model Representing the Geometrical Shielding of the Lunar Module, SD68-798, North American Rockwell Corporation, 1968.

[7] Mar, B. W.: Electron Shielding Codes for Evaluation of Space Radiation Hazards, D2-90414, The Boeing Company, Seattle, Washington, 1963.

[8] R-P&VE - VAW Program WP04A, 10/9/68: Current ATM Weights and Mass Characteristics, MSFC-NASA, 1968.

[9] Shelton, R. D.; deLoach, A. C.: Analysis of Radiation Damage to ATM Film, NASA TM X-53666, MSFC-NASA, 1967.

[10] Watts, J. W.: Film Degradation Resulting from Magnetically Trapped Protons in ATM Orbits, IN-SSL-N-69-2, MSFC-NASA, 1969.

[11] Watts, J.W.; Burrell, M. O.: Private Communication.

[12] Vette, J. I.: Models of the Trapped Radiation Environment, Vols. 1-3, NASA SP-3024, 1966-1967.